Published in final edited form as:
Dev Biol. 2008 December 1; 324(1): 161–176. doi:10.1016/j.ydbio.2008.09.002.

Wnt signaling is required for organization of the lens fiber cell cytoskeleton and development of lens three-dimensional architecture

Yongjuan Chen[1], **Richard J.W. Stump**[1,2], **Frank J. Lovicu**[1,2,3], **Akihiko Shimono**[4], and **John W. McAvoy**[1,2,*]

1*Save Sight Institute, The University of Sydney, NSW 2001, Australia*

2*Vision Cooperative Research Centre, Sydney, Australia*

3*Anatomy and Histology, Bosch Institute, The University of Sydney, NSW 2006, Australia*

4*Oncology Research Institute, National University of Singapore, Singapore 117456*

Abstract

How an organ develops its characteristic shape is a major issue. This is particularly critical for the eye lens as its function depends on having appropriately ordered three-dimensional cellular architecture. Recent in vitro studies indicate that Wnt signaling plays key roles in regulating morphological events in FGF-induced fiber cell differentiation in the mammalian lens. To further investigate this the Wnt signaling antagonist, secreted frizzled-related protein 2 (Sfrp2), was overexpressed in lens fiber cells of transgenic mice. In these mice fiber cell elongation was attenuated and individual fibers exhibited irregular shapes and consequently did not align or pack regularly; microtubules, microfilaments and intermediate filaments were clearly disordered in these fibers. Furthermore, a striking feature of transgenic lenses was that fibers did not develop the convex curvature typically seen in normal lenses. This appears to be related to lack of protrusive processes that are required for directed migratory activity at their apical and basal tips as well as for the formation of interlocking processes along their lateral margins. Components of the Wnt/Planar Cell Polarity (PCP) pathway were downregulated or inhibited. Taken together this supports a role for Wnt/PCP signaling in orchestrating the complex organization and dynamics of the fiber cell cytoskeleton.

Keywords

Lens development; Wnt signaling; Planar cell polarity; Lens fibers; Lens cell cytoskeleton; Rho GTPases; Frizzled; Secreted frizzled-related proteins

Introduction

How the eye lens develops its characteristic shape and three-dimensional cellular architecture is a major developmental question. Lens tissue differentiates from ectoderm situated next to

*Author for correspondence (e-mail:johnm@eye.usyd.edu.au).

the optic vesicle. By thickening and invaginating, the ectoderm forms the lens vesicle. Subsequently, posterior vesicle cells elongate to form the primary fibers, whereas anterior vesicle cells differentiate into epithelial cells. The divergent fates of these embryonic cells give the lens its distinctive polarity. Once formed, the lens grows rapidly by cell division and differentiation. Cell proliferation occurs in the epithelial region just above the lens equator known as the germinative zone (McAvoy, 1978). Progeny of divisions migrate below the equator where they elongate and differentiate into secondary fiber cells. In this way, the lens grows throughout life and maintains its polarity.

Growth factors are key regulators of cell fates and behaviors and much attention has focused on identifying the factors that govern proliferation, migration and differentiation of lens cells. Initial studies with a mammalian lens epithelial explant system identified members of the FGF growth factor family as key regulators of lens fiber differentiation. Moreover, detailed analyses showed that FGFs could induce dose-dependent responses. Specifically, a low dose of FGF induced lens cell proliferation, whereas sequentially higher doses were required to induce epithelial cell migration and fiber cell differentiation (McAvoy and Chamberlain, 1989). This finding, together with the fact that FGF bioavailability differs throughout the eye (e.g. more FGF can be recovered from the vitreous than aqueous; Schulz et al., 1993), led to the hypothesis that the distinct polarity of the lens in the eye is determined by a gradient of FGF signaling. Subsequent genetic manipulations with the murine lens, where FGFs were overexpressed or FGF receptors were knocked out, have now provided compelling evidence for this hypothesis (Lovicu and McAvoy, 2005; Robinson, 2006; Zhao et al., 2008). However, it has become increasingly clear from both in vitro and in vivo studies that mammalian fiber differentiation also depends on a FGF-initiated cascade of growth factor signaling involving other growth factor-dependent pathways (de Iongh et al., 2001; Faber et al., 2002; Belecky-Adams et al., 2002; Lovicu and McAvoy, 2005; Boswell et al., 2008). Most recently, there is evidence that members of the Wnt family play key roles in regulating events in fiber differentiation in the mammalian lens (Lyu and Joo, 2004; Chen et al., 2006).

Wnt signaling is initiated when a Wnt ligand complexes with a frizzled (Fz) receptor and a LDL-related protein (Lrp) co-receptor. Once this complex is formed, dishevelled (Dvl) is activated and axin is recruited to the cell membrane. In the absence of Wnt, axin is part of a module containing glycogen synthase kinase-3β (GSK3β) that phosphorylates β-catenin and targets it for destruction (Cong et al., 2004; Logan and Nusse, 2004). Thus ligand/receptor interaction leads to an increase in stabilized (unphosphorylated) β-catenin. In this form, β-catenin can then associate with the DNA binding transcription factors TCF or Lef, and in the nucleus regulate expression of target genes. Other, non-canonical Wnt signaling pathways have also been identified, and these include the Wnt/Ca^{++} and the Wnt/planar cell polarity (PCP) pathways (Karner et al., 2006; Jones and Chen, 2007). Although not as well understood as canonical Wnt signaling, there is a growing awareness that non-canonical signaling, particularly through the Wnt/PCP pathway, has a critical role in regulating many key developmental processes that involve intricate remodeling of the cell cytoskeleton. For example, the elongation and narrowing of tissues, or convergent extension movements, that are fundamental to critical processes such as gastrulation and neurulation involve highly coordinated cellular shape changes and rearrangements that are driven by Wnt/PCP signaling (Green and Davidson, 2007). Wnt signaling through the PCP pathway involves activation of Dvl, although through a different domain(s) than for canonical signaling, and generally involves activation of the small Rho GTPases and results in the activation of JNK (Logan and Nusse, 2004; Wallingford and Habas, 2005; Karner et al., 2006; Jones and Chen, 2007).

Wnts, their Fz receptors and Lrp5/6 co-receptors are expressed in the mammalian lens during development (Stump et al., 2003; Liu et al., 2003; Chen et al., 2004 Ang et al., 2004). In previous studies we showed that mouse embryos homozygous for a mutation in the *lrp6* gene that have

impaired Wnt/β-catenin signaling did not form a normal lens (Stump et al., 2003). This defect was evident at E13.5 when cells of the anterior region of the lens vesicle did not normally differentiate into a polarized sheet of adherent epithelial cells, but instead accumulated the fiber-specific marker, β-crystallin, and extruded into the corneal stroma. Results from TCF/Lef-LacZ reporter mice also show a period of Wnt/β-catenin reporter activity in the lens epithelium at this time (between E11.5–14.5; Liu et al., 2003, 2006, 2007). Taken together this indicates a requirement for Wnt/β-catenin signaling between E11.5–14.5 for the lens epithelium to differentiate from the anterior cells of the lens vesicle.

For lens fibers, explant studies indicate a role for Wnt signaling in mediating FGF-triggered fiber differentiation (Lyu and Joo, 2004). Fiber differentiation in vivo is unlikely to involve canonical Wnt signaling as no TCF/Lef-LacZ reporter activity is detected in any part of the lens beyond E14.5 (Liu et al., 2003, 2006, 2007). However, given that Wnt/PCP core signaling components Prickle and Van Gogh-like (Bekman and Henrique, 2002; Tissir and Gofinet, 2006) as well as Fzs and Dvls (Stump et al., 2003; Liu et al., 2003; Chen et al., 2004; Ang et al., 2004; Lyu and Joo, 2004) are prominent in elongating mammalian fiber cells, this effect may be mediated through the PCP pathway. In particular, Wnt/PCP signaling may have a role in mediating the effects of FGF in promoting the complex cytoskeletal reorganization required for the transition of epithelial cells into elongated, highly ordered fiber cells (Chen et al., 2006). A role for Wnt/PCP signaling in this process is consistent with studies that show impairment of the fiber cell cytoskeleton is a consequence of inhibiting the small Rho GTPases (Maddala et al., 2001, 2004; Rao et al., 2002). However, whilst these studies have identified roles for these GTPases in fiber cell elongation, it is not clear in this context if their activity is related to Wnt/PCP signaling.

The aim of the current study was to assess the role of the Wnt/PCP pathway in lens fiber differentiation by blocking Wnt signaling in the lens. To achieve this we overexpressed (using a lens crystallin promoter) the Wnt signaling antagonist, secreted frizzled-related protein 2 (Sfrp2), in the lenses of transgenic mice. Sfrps antagonize Wnt cascades by binding to Wnts or Fz receptors (Kawano and Kypta, 2003), and have the potential to modulate Wnt signaling activity in cells through all Wnt signaling pathways (Jones and Jomary, 2002). Although all five *Sfrp* genes are expressed during lens development (Chen et al., 2004), *Sfrp2* was selected for this transgenic study because, unlike the other *Sfrp* genes, it has a distinctive expression pattern early in lens morphogenesis that coincides with regions where inactivation of Wnt signaling is required for normal lens development (Smith et al., 2005). Evidence that Sfrp2 can inhibit Wnt signaling also comes from studies in various other systems (Lescher et al., 1998; Ladher et al., 2000; Deb et al., 2007) and recently a plethora of studies have linked Sfrp2 inhibition of Wnt signaling with an important tumor suppressor function (Nojima et al., 2007).

Results from the current study have shown that overexpression of Sfrp2 in fiber cells of transgenic mice led to the development of severe cataracts. Lens fiber elongation was attenuated and at their anterior and posterior tips they did not migrate towards the lens poles to form sutures. As a result fibers did not develop the characteristic convex curvature that is central to the development of normal three-dimensional lens architecture. Microtubules, microfilaments and intermediate filaments were disorganized in the incipient fiber cells of these transgenic mice. In addition, components of the PCP pathway, including Dvl, Cdc42, Rac1, RhoA and JNK were disturbed and, in the case of Dvl and the small GTPases, were downregulated/inhibited. Taken together this supports a role for Wnt/PCP signaling in regulating the complex organization of the cytoskeleton that is required for normal lens fiber differentiation and maturation.

Materials and Methods

Animals

The use of animals in this study conformed to the Association for Research in Vision and Ophthalmology (ARVO) Statement for the use of animals in Ophthalmic and Vision Research. Mutant mice deficient for Sfrp2 were generated as previously described (Satoh et al., 2006).

Construction of the plasmid with the Sfrp2 full-length gene

Full length *Sfrp2* cDNA (U88567 in GenBank) was sub-cloned into the δ1αA crystallin promoter plasmid (provided by Dr. Reneker, University of Missouri, USA) that consisted of a modified mouse αA-crystallin promoter, the chick δ1-crystallin enhancer element and the human growth hormone polyadenylation (polyA) region (Fig. 1H; Reneker et al., 2004).

Generation of transgenic mice and genotyping

The Sfrp2 transgene was injected into pronuclei of one-cell-stage BCBF1 (C57/BL6xCBA) mouse embryos by the Transgenic Animal Service of Queensland (Queensland, Australia). Transgenic mice were genotyped by PCR using primers specific for the *Sfrp2* transgene (forward: 5'tcgctagtccacgatgcc3'; reverse: 5'actgggaaactagcattgca3') or the δ1-crystallin enhancer (forward: 5'gctgacgcaaaaatccctaatg3'; reverse: 5'caggaaataccaacttctgccatc3'). Total RNA was extracted from 5-day-old postnatal lenses (P5) of Sfrp2 overexpressing transgenic mice or WT littermates as described previously (Chen et al., 2004). Briefly, 2 μg of RNA treated with DNAase I was reverse transcribed, with or without reverse transcriptase, for PCR amplification using specific primer pairs to amplify Sfrp2. To genotype littermates from heterozygotic Sfrp2 matings, PCR amplification using genomic DNA from crude tail digests was performed using DirectPCR (Viagen Biotech CA, USA) as described above.

Tissue collection and histology

Embryos at embryonic day 12.5 (E12.5), E14.5, E16.5 or eyeballs at P1 and P21 of Sfrp2 transgenic mice and WT littermates were fixed in 10% neutral buffered formalin (NBF) overnight, or with HistoChoice (Amresco, OH, USA) for 2 hours at room temperature. Tissues were dehydrated through a graded ethanol series, cleared in xylene and embedded in paraffin wax. All tissues were sectioned at 5μm and stained with haematoxylin and eosin.

Transmission electron microscopy (TEM)

The lenses from transgenic mouse line Sfrp2-m2 and WT littermates at P1 were fixed in 4% paraformaldehye/2% glutaraldehyde in 0.1M cacodylate buffer, pH 7.4, for 3 hours at room temperature. After washing and postfixation with 1% osmium tetroxide in phosphate buffer, the lenses were stained in 2% uranyl acetate and embedded in Epon-Araldite resin. Sections were stained and viewed on a 7100FA transmission electron microscope (Hitachi Koki, Tokyo, Japan).

In situ hybridization

In situ hybridization was conducted with a dioxygenin (DIG)-labeled Sfrp2 riboprobe as described previously (Chen et al., 2004). In brief, DIG-labeled complementary antisense and sense RNA probes were transcribed from the linearized plasmid templates containing the *Sfrp2* gene using *SP6* or *T7* RNA polymerases, respectively, and DIG-labeled nucleotides using a labeling kit (Roche, Mannheim, Germany). The expression patterns of the *Sfrp2* gene were examined by *in situ* hybridization on paraffin sections of E12.5 WT lens and embryonic and postnatal Sfrp2 transgenic lenses.

Immunohistochemistry

Sections of E14.5, P1 and P21 lenses from Sfrp2 transgenic and WT mice were deparaffinized in xylene and hydrated through a graded ethanol series to PBS. The slides were blocked with rabbit or goat serum for half an hour and incubated with primary antibodies overnight at 4°C. The primary antibodies used were specific for α-tubulin and acetylated α-tubulin (Sigma, MO, USA), Sfrp2, Cdc42, Rac1, RhoA, phospho-JNK (pJNK), (all from Santa Cruz Biotechnology, CA, USA) and filensin (provided by Roy Quinlan, University of Durham, UK). For controls, non-immune serum was substituted for the primary antibody. The sections were incubated with the secondary antibody conjugated with Alexa 488 for one hour at room temperature and visualized by confocal microscopy (Zeiss LSM 5 PASCAL; Carl Zeiss, NSW, Australia). Phalloidin conjugated with Alexa 488 (Invitrogen Australia Pty, Ltd) was used to localize F-actin. In some cases, the sections were counterstained with propidium iodide (PI, Molecular Probes, CA, USA).

Western blotting

Whole lenses were dissected from Sfrp2 transgenic mice or WT littermates at P5. For the extraction of soluble proteins (SP) and insoluble proteins (ISP), the lenses were lysed in ice-cold lysis buffer CSK (0.5%Triton, 50mM NaCl, 300 mM sucrose, 10 mM PIPES, 3 mM $MgCl_2$, 1 mM Na_3VO_4, 10 mM $Na_4P_2O_7$, 50 mM NaF) supplemented with protease inhibitor (Complete Mini, Roche). The homogenized mixture was then centrifuged at 16000 × g for 20 minutes at 4°C to separate the soluble protein from insoluble protein. The supernatant containing the soluble extract was collected as SP. The remaining pellet was then treated with SDS buffer (10 mM Tris HCl, 2 mM EDTA, 1% SDS, 1 mM Na_3VO_4, 0.1 mM Octyglucoprynaoside) supplemented with protease inhibitor. The mixture was vortexed and then centrifuged at 16000 × g for 20 minutes. The supernatant containing the soluble extract was collected as ISP. Total proteins were extracted from the whole lenses of Sfrp2-m2 transgenic mice and WT littermates at P5 using RIPA lysate buffer (Sigma). Lens tissue was homogenized with a pestle and followed by brief treatment with a microprobe sonicator. The homogenized tissues were then centrifuged at 16000 × g for 20 minutes at 4°C. The SP, ISP and total proteins were quantified with a protein assay dye reagent kit (Bio-Rad Laboratories, Hercules, Canada).

Western blotting was carried out as previously described (Stump et al., 2003). Primary antibodies for the small GTPases and pJNK were as for immunohistochemistry. Antibodies for PAK, phospho-PAK1/2 and Dvl3 (Cell Signaling Technology, MA, USA), Dvl2 (Santa Cruz), Fz3 (R&D Systems, MN, USA) and GAPDH (HyTest Ltd, Finland) were also used. Following application with a secondary antibody conjugated with horseradish peroxidase (HRP) (1:25000) (Upstate, VA, USA), and ECL (Pierce, IL, USA), band density was assessed or measured using Scion Image software (Scion Corporation, MD, USA). For quantification three separate lysates were used and results analyzed with StatsDirect (UK) and graphed with SigmaPlot Version 9.1 (Systat Software, Inc, USA).

Immunoprecipitation

Total proteins for immunoprecipitation were extracted as above. For pre-clearing the lysates, 1000–1200 μg total proteins from WT or Sfrp2-m2 lens lysates were incubated with 0.25 μg rabbit IgG (Zymed Laboratories, CA, USA) for one hour at 4°C on a shaking table. Then 20 μl of protein A/G agarose beads (Santa Cruz) was added into the mixture and incubated for 30 minutes at 4°C on a shaking table. Agarose beads were centrifuged at 12000 × g for 10 seconds at 4°C to pellet the beads. The supernatant was collected in a new tube on ice for immunoprecipitation. The primary antibody was then added (0.2–2 μg anti-Sfrp2) along with 20 μl of agarose beads into the pre-cleared lysates and incubated at 4°C overnight on a shaking table. The agarose beads were then collected by spinning at 1000 × g for 30 seconds at 4°C.

The beads were washed 2–4 times in RIPA buffer. The centrifugation and washing steps were then repeated after each wash. The agarose beads were then resuspended in 20 μl of 2×sample buffer, boiled for 2–3 minutes to denature proteins and stored on ice prior to loading on SDS-PAGE gel for western blotting using antibodies for Sfrp2 and Wnt7b (Santa Cruz).

Results

Gross morphology of Sfrp2 transgenic lenses

With the overall aim of identifying roles for Wnt signaling in lens development, transgenic mice were generated that overexpressed the Wnt signaling antagonist, Sfrp2, in the eye. Two transgenic lines of mice were generated that overexpressed the Wnt signaling antagonist, Sfrp2, in the eye. Both lines exhibited ocular phenotypes, with severe bilateral cataracts in Sfrp2-m1 (Fig. 1B) and microphthalmia in Sfrp2-m2 (Fig. 1C). Removal of lenses at P5 showed that, compared with WT littermates, lenses from Sfrp2 transgenic mice were opaque (Fig, 1D, E, F). Transgenic lenses were smaller than WT lenses (Fig. 1E, F). Lenses from the Sfrp2-m2 line were often abnormal in shape and had a ruptured posterior capsule.

RT-PCR was employed to check transgene expression in the lenses. Total RNA was extracted from lenses of P5 Sfrp2 transgenic and WT littermates. RT-PCR showed that the *Sfrp2* transgene (910 bp) was expressed in the lenses of both Sfrp2-m1 and Sfrp2-m2 mice, but not in WT lenses (Fig. 1G). The presence of the chick δ1-crystallin enhancer gene (565 bp) in genomic DNA was used to identify transgenic mice in litters from heterozygotic Sfrp2 matings (Fig. 1G).

Patterns of Sfrp2 expression in transgenic lenses

mRNA expression—In situ hybridization studies showed that Sfrp2 mRNA was expressed weakly in the presumptive lens epithelium in WT lenses at E12.5, but was absent from the primary fibers. Expression was also evident in the optic cup but tended to be reduced or absent at the margins (Fig. 2A). This is the pattern of expression that is characteristic of endogenous Sfrp2 at this stage of development (Chen et al., 2004). In the Sfrp2-m1 lens at E12.5, in addition to weak expression in the lens epithelium, Sfrp2 mRNA was prominently expressed in the lens primary fibers (Fig. 2B). The Sfrp2-m2 lens showed a similar pattern of expression at this stage (not shown). At P21, Sfrp2 mRNA was still very strongly expressed in elongating cells at the lens equator and in cortical fiber cells of the Sfrp2-m1 lens (Fig. 2C). Sfrp2 transcripts were only weakly, if at all, expressed in the epithelial cells above the lens equator in these lenses (Fig. 2C, arrow). The Sfrp2-m2 lenses, at P21, showed a similar pattern of expression except that expression appeared to be stronger than in Sfrp2-m1 lenses (Fig. 1D).

Protein expression—At E14.5, strong immunoreactivity for Sfrp2 was evident in the fiber cells of Sfrp2 lenses and was weak or undetectable in epithelial cells (Fig. 2E). Similarly at P21, Sfrp2 protein was strongly localized in the elongating cells at the lens equator and in the cortical fiber cells of Sfrp2 lenses (Fig. 2F). Western blotting showed that Sfrp2 protein (33 kDa) was present predominantly in the insoluble fraction from Sfrp2-m1 lenses at P5. By this method Sfrp2 protein was undetectable in postnatal WT lenses (Fig. 2G). The insoluble protein mainly represents membrane and nuclear proteins. The observation that Sfrp2 was substantially greater in the insoluble, compared with the soluble, fraction is consistent with Sfrp localization to plasma membranes and/or the extracellular matrix when synthesized by cultured cells (Kawano and Kypta, 2003). Taken together with the in situ results this shows that Sfrp2 protein remained localized to the cells that produced it.

Sfrp2 protein co-precipitates with Wnt7b—As the Sfrps are extracellular antagonists that modulate Wnt signaling pathways by ligand-receptor interactions, we wanted to determine

if the overexpressed Sfrp2 associated with any Wnt ligands. As Wnt7b is prominently expressed in the lens (see Stump et al., 2003; Ang et al., 2004; Lyu and Joo, 2004) and antibodies for Wnt7b were available, we immunoprecipitated Sfrp2 from homogenates of WT and transgenic lenses, followed by SDS-PAGE immunoblotting for Wnt7b. A strong band for Sfrp2 was detected in the immunoprecipitate from transgenic lenses and immunoblotting revealed that this contained abundant Wnt7b (Fig. 3). In contrast, only traces of Sfrp2 and Wnt7b were detected in the immunoprecipitate from WT mice.

Histological analysis of the Sfrp2 transgenic lenses

To investigate the structural changes in transgenic lenses, heterozygous transgenic mice were mated to generate homozygous, heterozygous and WT littermates. Eyeballs from P21 Sfrp1-m1, Sfrp2-m2 and WT littermates were sectioned and stained with H&E. In WT lenses, the elongating and maturing fibers showed orderly alignment along the fiber axis in the transitional zone (Fig. 4A, $4A_2$). In contrast, the lenses of Sfrp2-m1 mice had severely disrupted cellular architecture (Fig. 4B, $4B_2$). The lenses in Sfrp2-m1 mice were smaller in size than the lenses of WT controls (compare Figs. 4A and 4B). The epithelial cells appeared to be normally arranged but tended to have larger nuclei (Fig. $4B_1$) compared to epithelial cells in WT lenses (Fig. $4A_1$). In lenses of Sfrp2-m1 mice the fibers in the transitional zone initially exhibited normal elongation, but, as differentiation progressed, they became disorganized. In the lens cortex, where fiber cell maturation occurs, fiber cells often appeared very disorganized and large vacuoles, or inter-cellular spaces, were abundant (Fig. $4B_2$). In the lens nucleus, the fibers had lost their characteristic structure and were often completely broken down (Fig. 4B, asterisk). Degeneration of fibers was usually accompanied with rupture of the posterior capsule (data not shown).

Consistent with their smaller size, the lenses from Sfrp2-m2 mice showed a more pronounced disruption to the fiber mass than in lenses of Sfrp2-m1 mice (Fig. 4C). In the Sfrp2-m2 lens, fiber differentiation was clearly inhibited and in the center of the lens a large lumen underneath the epithelium was evident (Fig. 4C, $4C_2$, asterisk). One of the most striking features of Sfrp2-m2 lenses at P21 was that, although fiber elongation was initiated at the transitional zone, the differentiating fibers did not elongate sufficiently to contact or maintain contact with the epithelial layer (Fig. $4C_2$). In Sfrp2-m2 lenses, the epithelium was generally reduced in size. The phenotype of the epithelial cells varied between lenses. In most cases cells were vacuolated and occasionally some epithelial cells were seen to have detached and migrated into the fiber mass (Fig. $4C_1$).

Because of the severe disruption to the fibers in the postnatal Sfrp2 lenses further analysis of the phenotype was extended to include embryonic stages in order to identify the earliest point of divergence from normal development. For this, the Sfrp2-m2 line was studied because it exhibited the most severe phenotype.

Lenses were collected from E14.5, E16.5 and P1 Sfrp2-m2 and WT mice. Histological analysis showed that, at E14.5, the lenses in Sfrp2-m2 mice had essentially normal features in the epithelial and fiber cell compartments and could not be distinguished from the WT lens (compare Fig. 5B and 5A). At E16.5 the Sfrp2-m2 lenses were slightly smaller than lenses from WT littermates. The fibers in the Sfrp2-m2 lenses appeared to be less tightly packed than in the lenses of WT littermates (compare Fig. 5D and 5C). Also, fibers did not curve towards the developing sutures as they did in WT lenses (Fig. 5; black lines are included to emphasize curvature of fiber cells). Note that in both Sfrp2-m2 and WT lenses at the lens equator the elongating fibers in the transitional zone had a concave curvature i.e. relative to the surface of the lens (Fig. 5C, 5D). In WT lenses, as the fibers elongated, they migrated at their anterior and posterior tips along the epithelium and posterior capsule, respectively. During this process they progressively developed convex curvature, somewhat similar to the curvature of the whole

lens. Eventually they met up with equivalent fibers from an opposing segment of the lens and formed rudimentary sutures (Fig.5C, asterisks). However, in the Sfrp2-m2 lenses, the fibers retained a concave curvature, did not meet up with equivalent fibers from an opposing segment of the lens and did not form sutures (Fig. 5D). Later at P1, this lens fiber phenotype was even more pronounced. At this stage it is clear that fiber elongation in Sfrp2-m2 lenses had not progressed at the same rate as in WT lenses (compare Fig. 5F with 5E). Also the concave curvature of the fibers in the sfrp2-m2 lenses was even more pronounced than at earlier stages. A striking feature of the elongating fibers in the Sfrp2-m2 lenses was that, compared with WT lenses, they tended to remain at right angles to the posterior capsule (and to the epithelium when they were in contact with this layer; compare Fig.5E and 5F). In addition, and consistent with their abnormal fiber cell curvature, the lenses of sfrp2-m2 transgenic mice did not develop the curvature that is characteristic of the WT lens.

Although at P1 the epithelial sheet in the Sfrp2-m2 lenses was reduced in size compared with WT lenses, the epithelial cells appeared similar to those in WT lenses (compare Fig. 5F and 5E). Given that no epithelial phenotype was detected at earlier stages when a fiber phenotype was evident this indicates that the initial effect of overexpressing Sfrp2 in the lens was to disturb the differentiation and maturation of the fibers. This is consistent with the Sfrp2 protein being strongly localized to fiber cells and little, if any, present in epithelial cells (see Fig. 2).

Ultrastructural changes in the cells of Sfrp2 transgenic lenses

In light of the histological findings reported above, further investigation of the morphology of fibers from Sfrp2-m2 and WT mice was undertaken using transmission electron microscopy. Lenses from Sfrp2-m2 and WT littermates were collected at P1 and processed for electron microscopy. In WT lenses, the elongating lens fibers in the cortex were characteristically aligned and arranged in orderly rows along the anterior-posterior lens axis (Fig. 6A). In contrast, the fibers in the Sfrp2-m2 lenses were shorter and because of their more irregular shapes appeared less regularly aligned than fibers in WT lenses (Fig. 6B). Transverse sections of the lens fibers also showed that, whilst Sfrp2-m2 fibers were tightly packed they had reduced numbers of interlocking processes, such as ball-and-socket joints, that are abundant in normal fiber cells (Fig. 6, insets in A and B). In addition, small electron dense granules, mostly contained within vesicles, were abundant in some regions of the fibers of Sfrp2-m2 lenses but were not present in WT fibers (Fig. 6A, 6B, insets).

As noted above, the fibers in Sfrp2-m2 lenses showed no evidence of migration anteriorly or posteriorly, along the overlying epithelium or posterior capsule, respectively. Consistent with this the ultrastructural analysis revealed no evidence of protrusive processes at the anterior or posterior tips of the fibers in Sfrp2-m2 lenses (Fig. 7C, D). In WT lenses, protrusive processes were common at the anterior and posterior tips of the elongating fibers in the lens cortex. Anteriorly, short processes extended along the anterior face of the epithelium. Interlocking processes between fibers were also abundant in this region (Fig 7A). Posteriorly, long filopodia-like processes extended along the posterior capsule (Fig. 7B).

Disruption of cytoskeletal architecture in Sfrp2 transgenic lenses

Overexpression of *Sfrp2* in the lens of transgenic mice resulted in severe disruptions to the organization and morphology of lens fiber cells. To gain insights into the status of the cytoskeleton in these lenses, immunohistochemistry for α-tubulin, F-actin and filensin was used to localize components of microtubules (MTs), microfilaments (MFs) and beaded filaments (BFs), respectively.

Alpha-tubulin—In WT lenses at P1, α-tubulin was localized throughout the lens (Fig. 8A). At higher magnification, alignment of α-tubulin-labeled MTs could be discerned extending

along the elongating fiber axis (Fig. 8A_1). In contrast to WT lenses, α-tubulin reactivity in Sfrp2-m2 lenses was patchy and generally weaker. In addition, aligned MTs were not evident as in WT lenses (Fig. 8B, B_1). Note that, as a positive control, α-tubulin was strongly reactive in the neural retina of Sfrp2-m2 mice.

In MTs, α-tubulin undergoes several post-translational modifications. The modified tubulin usually accumulates in the stable pool of MTs (Palazzo et al., 2003). Acetylation is one of these modifications and acetylated α-tubulin is often used as an indicator of stabilized MTs. In WT lenses at P1, acetylated α-tubulin was strongly detected in the cortical fibers (Fig. 8C). Reactivity for acetylated α-tubulin was weak in the peripheral region of the epithelium but increased during fiber cell elongation in the transitional zone (Fig. 8C). In lenses of Sfrp2-m2 mice, reactivity for acetylated α-tubulin was weak and predominantly present in scattered patches (Fig. 8D). Similar to WT lenses, Sfrp2-m2 lenses revealed strong acetylated α-tubulin reactivity in the retina/ciliary body and this served as a useful positive control.

F-actin—Fluorescent-tagged phalloidin was used to localize F-actin. In both WT and Sfrp2-m2 lenses, there was strong localization of F-actin in both epithelial cells and fiber cells. Actin filaments were evident particularly along the margins of the cells in the lens cortex. Strong fluorescence was also evident at the epithelial-fiber interface and, to a lesser extent, along the base of the elongating fibers (Fig. 8E, F). Whilst the strength of fluorescence for F-actin was generally similar in WT and Sfrp2-m2 mice, a major difference was that in Sfrp2-m2 mice no undulations or interlocking processes were evident along their fibers. These were prominent in the inner cortical fibers of WT lenses (insets in Fig. 8E, F).

Filensin—In WT lenses reactivity for filensin was evident at the lens equator in the transitional zone where fiber cell elongation commences (Fig. 8G, arrow). In the fibers, filensin reactivity was present in prominent tramline-like arrangements that ran along their length (Fig. 8G, inset). In contrast, in the incipient fibers of Sfrp2-m2 lenses, filensin reactivity tended to be present in disorganized clumps and showed little tramline-like alignment (Fig. 8H, inset).

Changes in Wnt/PCP signaling components in Sfrp2 transgenic lenses

As noted in the Introduction, Wnt/PCP signaling through small Rho GTPases and activation of the JNK cascade is frequently a critical factor in cytoskeletal reorganization in many cellular contexts (Fenteany et al., 2000; Habas et al., 2003; Hall, 2005). Given the severe disruption of the cytoskeleton in Sfrp2-m2 lenses described above, the components of this pathway were investigated to determine if their expression and/or activity were also disturbed.

Cdc42 localization—In WT lenses, Cdc42 was similarly strongly localized in lens epithelial cells and cortical fiber cells (Fig. 9A). Immunoreactivity for Cdc42 was particularly strong at the basal ends of the elongating fibers at the lens equator (arrows). In the more mature fibers in the lens nucleus, reactivity tended to be weaker. In Sfrp2-m2 lenses, Cdc42 reactivity was substantially weaker than in WT lenses (Fig. 9B). In the fibers, only weak patches of Cdc42 reactivity were evident and at the lens equator, in contrast with the WT lenses, Cdc42 was barely detectable (Fig. 9B, arrows).

Rac1 localization—In WT lenses, Rac1 was strongly localized in the lens epithelial cells and fiber cells (Fig. 9C). Immunoreactivity was generally strong throughout all the fiber cells. Rac1 reactivity was also present in some of the fiber cell nuclei. In Sfrp2-m2 lenses, Rac1 reactivity was present throughout the lens but was generally weaker, particularly in the elongating cells at the lens equator (Fig. 9D, asterisk).

RhoA localization—In WT lenses RhoA was strongly localized in the lens epithelial and fiber cells. Immunoreactivity was particularly strong in the basal regions of elongating fibers at the lens equator (Fig. 9E, arrows). In Sfrp2-m2 lenses immunoreactivity was generally weaker throughout the lens compared with the WT (Fig. 9F).

pJNK localization—An antibody specific for the activated form of JNK (phosphorylated on Thr-183 and Tyr-185 residues) showed strong pJNK immunoreactivity localized to the cytoplasm and the nuclei of both lens epithelial and fiber cells in WT lenses (Fig. 10A). Although present in the nuclei of all lens cells, the nuclear reactivity increased in the cells of the equatorial region during fiber elongation and differentiation. Reactivity also increased in this zone in the baso-lateral region; although strongest in the basal region of these cells, reactivity often extended along the length of these elongating fiber cells (Fig. 10A, small arrows). Reactivity for pJNK was also evident at the junction of the epithelium and fibers and at the basal region of epithelial cells (Fig. 10A, inset). Compared to WT lenses, the lenses of Sfrp2-m2 littermates exhibited generally weaker pJNK reactivity (Fig. 10B). The only places where reactivity for pJNK seemed to be comparable in intensity to the WT lenses, was in the narrow band where the fibers and epithelial cells were in contact and in the fiber cell nuclei (Fig.10B). Propidium iodide nuclear stain highlighted the presence of abundant retained nuclei throughout the Sfrp2-m2 lenses (Fig. 10D). In comparison, WT lens fiber cell nuclei were characteristically lost in the lens cortex and were absent from the lens nucleus (Fig. 10C).

Clearly the localization patterns of components of the Wnt/PCP pathway, the small Rho GTPases and pJNK, were altered in Sfrp2-m2 lenses compared with WT lenses. Essentially, compared with WTs, there was reduced expression of all three GTPases and pJNK in the Sfrp2-m2 lenses and, in particular, in most cases distinctly weaker reactivity was evident in the elongating cells at the lens equator. In order to further examine this difference, levels of expression of the small GTPases and pJNK in Sfrp2-m2 and WT lenses were assessed by western blotting.

Western analysis of GTPases and JNK—Total proteins were extracted from postnatal lenses of Sfrp2-m2 and WT littermates and equal amounts of protein were loaded onto gels for immunoblotting analysis. Levels of Cdc42, Rac1 and RhoA were reduced in Sfrp2-m2 lens preparations compared with WTs (Fig. 11A, B). These differences were significant for Cdc42, Rac1 and RhoA, respectively. However, pJNK did not show a significant difference in the blots of Sfrp2-m2 and WT lenses. This appears to contradict the immunolocalization study that showed reduced cytoplasmic reactivity in the cells of the transitional zone and cortex of Sfrp2-m2 lenses compared with WT lenses (Fig.10A, B). The apparent discrepancy between western and immunolocalization results for pJNK may be accounted for by the abundance of retained nuclei in the Sfrp2-m2 lenses that were also strongly reactive for pJNK (see Fig. 10D).

Western analysis of the GTPase effector, PAK—In order to determine if the reduced levels of Cdc42, Rac1 and RhoA in the lenses of Sfrp2-m2 transgenic mice resulted in their reduced activity, we assessed levels of members of the PAK family that are well known effectors of these GTPases (see Arias-Romero and Chernoff, 2008). In contrast to total PAK, phospho-PAK (the activated form) was much reduced in lenses of Sfrp2-m2 transgenic mice compared with WTs. This is consistent with reduced GTPase activity accompanying their reduced levels in the Sfrp2-m2 lens (Fig. 11C).

Western analysis of Dvl—To determine if the inhibition of Rho GTPases and JNK was a result of Sfrp2 inhibiting the Wnt/PCP pathway we compared the status of Dvl in lenses from Sfrp2-m2 and WT mice. Dvl characteristically shows up as two bands in western blots, the upper band being the phosphorylated (activated) form and the lower band being the unphosphorylated (inactive) form. The results showed that significantly more activated Dvl2

was present in WT than in Sfrp2-m2 lenses (Fig. 11C, D). In addition, the inactive form of Dvl2 was significantly increased in Sfrp2-m2 lenses in comparison with WT lenses (Fig. 11C, D). Whilst the total amount of Dvl2 (combined active and inactive) did not change significantly between Sfrp2-m2 and WT lenses, the relative amounts of active and inactive forms were substantially different; ratios of active to inactive Dvl2 in WT and Sfrp2-m2 lenses being approximately 11:1 and 2:1, respectively. This Dvl 'band shift' is a characteristic feature of inhibition of Wnt/Fz signaling (e.g. see Schlessinger et al., 2007). For Dvl3, in WT lenses the active form was prominent and was significantly reduced in Sfrp2-m2 lenses. The inactive form of Dvl3 was barely detectable in WTs and was undetectable in Sfrp2-m2 lenses. Western blots for Fz3 showed no significant difference in levels between WT and Sfrp2-m2 lenses; further evidence that reduced activation of Dvl in Sfrp2-m2 lenses could not be attributed to a general down turn in expression of Wnt signaling components.

Sfrp2 mutant lenses

This study clearly shows that overexpression of Sfrp2 in the lens brings about major disruptions to the fiber cell compartment. With this in mind it was important to determine if the absence of a functional *Sfrp2* gene would have any effect on lens development. Analysis of eye development of *Sfrp2* mutant mice revealed no differences from WT mice at any stage of development. Even at mature age there was no sign of cataract or any histological abnormalities in lenses from *Sfrp2* mutants (Fig. 12). As all five *Sfrp* genes are expressed in the lens there may be some redundancy in function. This appears to be particularly relevant for the closely related *Sfrp1* and *Sfrp2* genes as functional redundancy in their ability to regulate anteroposterior axis elongation has recently been reported (Sato et al., 2006).

Discussion

This study has shown that mice overexpressing the Wnt signaling antagonist, Sfrp2, in lens fiber cells, undergo impaired lens development and subsequently develop cataracts. Histological analysis showed that in the Sfrp2 transgenics the elongation of secondary fiber cells was attenuated such that many failed to make contact with the overlying epithelium. Fiber cells also exhibited irregular shapes and consequently did not align or pack regularly as in the normal lens. Analysis of the major cytoskeletal components showed that microtubules, microfilaments and intermediate filaments did not show the high level of organization that is characteristic of the normal lens. In the fiber cells of Sfrp2 transgenic mice there was little evidence of the protrusive processes that are required for migratory activity at their apical and basal tips as well as for the formation of interlocking processes between them. In addition, components of the PCP pathway, including Dvl, Cdc42, Rac1, RhoA and JNK were disturbed and, in the case of Dvl and the small GTPases, were downregulated/inhibited. Taken together this supports a role for Wnt/PCP signaling in regulating the complex organization and dynamics of the cytoskeleton that is required for normal lens fiber differentiation and maturation.

The defect in the fiber cell compartment of the lens was the main feature of the phenotype of Sfrp2 overexpressing mice. Also importantly it was the earliest defect to be detected in these mice; first becoming evident at E16.5 by the lack of development of appropriate curvature of the lens fibers. At these early stages all other parts of the lens, including the epithelium, appeared normal. It was only at postnatal stages that epithelial defects were detected. This is consistent with overexpression of Sfrp2 mRNA being restricted to the lens fibers. In addition, the localization of Sfrp2 protein was largely restricted to the fibers at all embryonic and postnatal stages examined (see Fig. 2E and F). Therefore it appears that the cells that were primarily affected by the Sfrp2 transgene were the cells that were actively expressing it. Other studies have shown that Sfrps bind strongly to the cell surface (Finch et al., 1997; Uren et al., 2000; Kawano and Kypta, 2003). The current study also showed in western blots that most of

the Sfrp2 was in the insoluble fraction of the lens lysate and this is consistent with it being predominantly present in the membrane fraction (see Fig. 2G). Based on these considerations, particularly on the observation that fibers show the earliest defects, it appears likely that later defects such as those in the epithelial compartment of lenses of Sfrp2 overexpressing postnatal mice are a secondary effect of the disruption of the fiber cell mass rather than a direct effect of exposure to Sfrp2.

A role for Wnt/PCP signaling in fiber differentiation

Up to now the canonical Wnt signaling pathway has been the focus of most attention in lens development studies. This has been facilitated by the availability of three reporter lines of mice and these have been used to monitor canonical Wnt signaling in studies of various aspects of eye development. Significantly, analysis of reporter activity in TOP-gal (Miller et al., 2006), BAT-gal (Kreslova et al., 2007) and TCF/Lef-LacZ (Liu et al., 2006) mice have shown that canonical Wnt signaling is absent during lens induction and early stages of lens morphogenesis. This is consistent with evidence that canonical Wnt signaling is incompatible with the processes of early lens development (Smith et al., 2005; Kreslova et al., 2007). However, once the lens vesicle has formed the reporter studies indicate a short phase of canonical Wnt signaling that is restricted to the anterior cells of the lens vesicle from E11.5 to E14.5 (Liu et al., 2003, 2006, 2007). This phase of activity appears to be important for the formation of the lens epithelium from the anterior cells of the lens vesicle as Lrp6 mutant mice with impaired canonical Wnt signaling do not form a normal epithelial sheet (Stump et al., 2003). Beyond E14.5, as lens development proceeds, there is no evidence of reporter activity in any part of the lens indicating that canonical Wnt signaling plays no further part in the differentiation or maintenance of lens epithelial or fiber cells. On the other hand in vitro studies with lens epithelial explants (Lyu and Joo, 2004) and explanted whole lenses (Liu et al., 2006) have shown that given appropriate stimuli, such as exposure to lithium, canonical signaling can be detected in lens cells. In this context it is noteworthy that, in the case of the whole lens explant study, there was no evidence of canonical Wnt signaling in the absence of such stimuli (Liu et al., 2006). This indicates, as do all the reporter studies, that canonical Wnt signaling is not a feature of the normal process of fiber differentiation in vivo. Alternatively, it is possible that a low level or short phase of canonical signaling is involved in fiber differentiation and that enhancement of this process by exogenous stimuli, such as in the above studies, is needed for activity to reach detectable levels. Further studies may help to resolve this issue.

Unlike the case for the canonical pathway there is now growing evidence for a role for noncanonical Wnt signaling in regulating events in fiber differentiation, particularly the morphological processes involved in migration and elongation. Lens epithelial explant studies have identified a role for non-canonical Wnt signaling in promoting FGF-induced fiber cell elongation (Lyu and Joo, 2004). Similar studies in our laboratory raised the possibility that FGF-induced reorganization of the cytoskeleton during the transition of epithelial cells in highly elongated fibers is mediated by the Wnt/PCP pathway (Chen et al., 2006). Furthermore, core components of Wnt/PCP pathway including Prickle and Van Gogh-like have been localized in elongating mammalian fiber cells (Bekman and Henrique, 2002; Tissir and Gofinet, 2006; McAvoy et al., unpublished data). The current study now provides the first evidence for a functional link between Wnt/PCP signaling and the organization of the lens fiber cytoskeleton in vivo. This is primarily shown by the inhibition of Dvl in Sfrp2-m2 lenses. For both Dvl2 and Dvl3, their phosphorylated (activated) forms were substantially reduced in the lenses of Sfrp2-m2 mice compared with lenses from WTs. Also, at least, for Dvl2 the unphosphorylated (inactive) form was clearly more abundant in Sfrp2-m2 lenses than in WTs. Consistent with being downstream of Dvl, the Rho GTPases were downregulated and their effector PAK was clearly less active in Sfrp2-m2 lenses than in WTs. Moreover, phosphorylated (activated) JNK was reduced in the cytoplasm of the differentiating fiber cells.

These results fit with the growing number of studies that have implicated Dvl in GTPase regulation; for example, Wnt/Fz signaling mediated by Dvl activates Rho GTPases and through this regulates the dynamics and organization of actin and microtubules in dendrite development (Rosso et al., 2005). Also in scratch-induced migration, Dvl is required for the activation of a complex containing Cdc42 and this is required for organization of the microtubule cytoskeleton (Schlessinger et al., 2007). Interestingly, in a number of systems Dvl has been shown to co-localize with microtubules and actin (Krylova et al., 2000; Torres and Nelson, 2000; Capelluto et al., 2002). In the lens it will be important to determine if Dvl similarly co-localizes with cytoskeletal components and particularly important to determine if there is any accumulation/activation at sites where Rho GTPases and JNK are present and/or activated.

Polarized protrusive activity is an important feature of fiber differentiation

Clearly the normal differentiation of the relatively small (approximately 10 μm in height) epithelial cells into millimeter length fiber cells involves major reorganization of the lens cell cytoskeleton. At the lens equator, cells intercalate with one another to form highly ordered rows of elongating fibers, known as meridional rows. During fiber elongation, at least initially, there is little change in cell volume because the cells undergo narrowing and develop a ribbon-like morphology (Bassnett, 2005). Such changes are characteristic of convergent extension cellular movements that are integral to gastrulation, neurulation and tissue sculpting and that have been shown to be dependent on Wnt/PCP signaling (Green and Davidson, 2007). During fiber cell elongation, anterior and posterior fiber tips show protrusive activity as they migrate along the overlying epithelium and posterior capsule, respectively (see Fig. 7). Three-dimensional reconstructions of green fluorescing protein (GFP)-expressing cells have also shown that, consistent with protrusive activity, the fibers flatten out at their tips and filipodia-like processes are present basally (Bassnett, 2005; Shi and Bassnett, 2007). In this regard there is also a similarity with convergent extension movements as polarized protrusive activity is a key feature of cells involved in this process (Goto et al., 2005; Green and Davidson, 2007). Thus, as lens fiber cells continue to elongate and migrate, anterior and posterior tips of fibers from opposing segments of the lens eventually meet to form sutures. During this process the fibers change from concave to convex as they extend and bend around to meet fibers from the opposing hemisphere of the lens. A major finding in this study was that this process was inhibited in Sfrp2 overexpressing mice. The fibers in the Sfrp2 transgenic lenses, unlike their WT littermates, retained their concave curvature and exhibited no protrusive processes at their tips or any other evidence of migratory activity.

The importance of cytoskeletal dynamics in regulating protrusive activity associated with directed migration of elongating lens fiber cells has also been clearly shown by studies of Abi2 null mice (Grove et al., 2004). The Abl-interactor (Abi) family of adaptor proteins localizes to sites of actin polymerization and protrusive membrane structures and regulates actin dynamics. Abi2 is normally expressed at the tips of elongating fiber cells, particularly at the transitional zone where newly differentiating fibers begin their migration along the anterior surface of the epithelium. In the absence of Abi2, the fibers show no directed migration, retain a concave curvature and do not form sutures (Grove et al., 2004). This phenotype is first detected, as in our Sfrp2 transgenic mice, at E16.5 and similarly during postnatal development culminates in rupture of the posterior capsule and loss of the primary fibers. As with our Sfrp2 transgenic mice no epithelial defects are detected at these early stages. The striking similarities in the lens phenotypes of the Abi2 null and Sfrp2 transgenic mice are compelling and are strongly indicative of a common origin of the fiber cell defects. Likely targets of Abi2 are the Rho GTPases as the regulation of actin dynamics by the Abl family kinases has been shown to be mediated by these molecules (Zandy et al., 2007). Further support for this comes from the studies of Rao and colleagues who have used various strategies to inhibit Rho GTPases in the lens and shown that this leads to major disruption of the lens fiber cytoskeleton (Maddala et

al., 2004; Rao and Maddala, 2006), with similarities to that described for the Abi2 null and Sfrp2 overexpressing mice. Taken together these studies have clearly shown involvement of the Rho GTPases in the organization of the cytoskeleton during fiber differentiation. The current study now, for the first time, identifies a functional link between Wnt signaling and the Rho GTPases and JNK in their regulation of cytoskeletal dynamics and organization in lens fiber cells.

In addition, the current study has identified a link between Wnt signaling and the formation of the many interlocking processes that form along the lateral margins of elongated fibers and that are critical for maintaining their adhesion and alignment. Lack of interlocking processes in the Sfrp2 overexpressing mice fits with deficiencies in cytoskeletal dynamics and actin branching as described above. Earlier electron microscopy studies have shown that the abundant interlocking processes that are prominent along the lateral margins of the fibers show evidence of actin branching similar to that generally shown during the formation of protrusive processes associated with migration (Zhou and Lo, 2003). Therefore the relative absence of these interlocking processes in Sfrp2 mice is consistent with a general inhibition of formation of protrusive processes in the lens fiber cells both at their tips and along their lateral margins. Mediolateral protrusive activity is also a feature of cells undergoing convergent extension movements (Goto et al., 2005; Green and Davidson, 2007) and once again highlights the similarity between this process that is known to be driven by Wnt/PCP signaling and the elongation, narrowing and intercalation of differentiating lens fiber cells

Relationship between FGF and Wnt/PCP signaling

Whilst a number of growth factor signaling pathways have now been implicated in regulating aspects of the fiber differentiation process, all the evidence points to FGF signaling being necessary for initiation of this process (Lovicu and McAvoy, 2005; Robinson, 2006, Zhao et al., 2008). This raises the question of how Wnt/PCP signaling is activated by FGF. Studies in several other systems have shown links between the FGF and Wnt signaling pathways in general (Olivera-Martinez and Storey, 2007; Wahl et al., 2007) and the PCP pathway in particular (Voiculescu et al., 2007). One study has also shown that the establishment of a hindbrain-inducing centre depends on the activation of FGF/MAP-kinase signaling which then modulates the PCP pathway (Aamar and Frank, 2004). This fits with the situation in the lens as FGF-activated MAP kinases, ERK1/2, have been shown to be critical for progress of the morphological features of fiber cell differentiation (Lovicu and McAvoy, 2001). A number of other studies have also identified various links between Wnt and ERK pathways (Yun et al., 2005; Almeida et al., 2005; Kim and Choi, 2007). Therefore, in future studies it will be important to investigate the involvement of ERK in interactions between FGF and Wnt/PCP signaling in the lens.

Lenses of Sfpr2 overexpressing mice do not develop appropriate three-dimensional architecture

In addition to linking the Wnt/PCP signaling pathway with the many important events in organizing the cytoskeletal elements of the differentiating fiber cells, this study also serves to highlight the importance of the cytoskeleton in generating fibers with appropriate adhesive properties, length and curvature and how this relates to important properties of the lens. In relation to adhesion it was noted that the fiber cells in Sfpr2-m2 lenses readily came apart when the lens capsule was torn (data not shown). This is very unlike the situation with WT littermates that needed much teasing and tearing to even partially dissect out clumps of fibers. This is consistent with WT lenses having abundant interlocking processes that are important for providing stable associations between neighbouring fibers (Zhou and Lo, 2003). In relation to fiber cell length and curvature, it was noted that as a general feature, lenses of Sfrp2 transgenic mice tend to be a different shape than WT littermates. The most common characteristic is that

the anterior surface of the lens tends to lack the curvature that is typical of the normal lens and that is critical for its ability to focus light. This ‘flat top’ feature varied considerably between lenses but can be readily appreciated by comparing Figure 5F with 5E and Figure 8F with 8E. Currently little is known about the mechanisms that determine and modulate lens shape, particularly its curvature, during eye formation and growth. As the Wnt/PCP pathway is known to play key roles in coordinating cellular shape, movements and behaviour during the morphogenesis and sculpting of many tissues, further studies on this pathway in the lens may yield insights into at least some of the mechanisms involved in processes that are critical for the acquisition and maintenance of normal three-dimensional lens architecture.

Acknowledgements

The authors thank Diana van Driel for expert assistance with transmission electron microscopy and Sharyn Ang and Anke Nguyen for expert assistance with histology, western blotting and immunoprecipitation. This work was possible because of support from the Sydney Foundation for Medical Research; NHMRC (Australia), NIH (USA, R01 EY03177) and Ophthalmic Research Institute of Australia. This research was undertaken as part of the Vision Cooperative Research Centre, New South Wales, Sydney, Australia, supported by the Australian Federal Government through the Cooperative Research Centres Programme.

References

Aamar E, Frank D. Xenopus Meis3 protein forms a hindbrain-inducing center by activating FGF/MAP kinase and PCP pathways. Development 2004;131:153–163. [PubMed: 14660437]

Almeida M, Han L, Bellido T, Manolagas SC, Kousteni S. Wnt proteins prevent apoptosis of both uncommitted osteoblast progenitors and differentiated osteoblasts by beta-catenin-dependent and -independent signaling cascades involving Src/ERK and phosphatidylinositol 3-kinase/AKT. J. Biol. Chem 2005;280:41342–41351. [PubMed: 16251184]

Ang SJ, Stump RJ, Lovicu FJ, McAvoy JW. Spatial and temporal expression of Wnt and Dickkopf genes during murine lens development. Gene Expr. Patterns 2004;4:289–295. [PubMed: 15053977]

Arias-Romero LE, Chernoff J. A tale of two Paks. Biol. Cell 2008;100:97–108. [PubMed: 18199048]

Bassnett S. Three-dimensional reconstruction of cells in the living lens: the relationship between cell length and volume. Exp. Eye Res 2005;81:716–723. [PubMed: 15963502]

Bekman E, Henrique D. Embryonic expression of three mouse genes with homology to the Drosophila melanogaster prickle gene. Mech. Dev 2002;119:S77–S81. [PubMed: 14516664]

Belecky-Adams TL, Adler R, Beebe DC. Bone morphogenetic protein signaling and the initiation of lens fiber cell differentiation. Development 2002;129:3795–3802. [PubMed: 12135918]

Boswell BA, Lein PJ, Musil LS. Cross-talk between FGF and BMPs regulates gap junction-mediated intercellular communication in lens cells. Mol. Biol. Cell 2008;19:2631–2641. [PubMed: 18400943]

Capelluto DG, Kutateladze TG, Habas R, Finkielstein CV, He X, Overduin M. The DIX domain targets dishevelled to actin stress fibers and vesicular membranes. Nature 2002;419:726–729. [PubMed: 12384700]

Chen Y, Stump RJ, Lovicu FJ, McAvoy JW. Expression of Frizzleds and secreted frizzled-related proteins (Sfrps) during mammalian lens development. Int. J. Dev. Biol 2004;48:867–877. [PubMed: 15558478]

Chen Y, Stump RJ, Lovicu FJ, McAvoy JW. A role for Wnt/planar cell polarity signaling during lens fiber cell differentiation? Semin. Cell Dev. Biol 2006;17:712–725. [PubMed: 17210263]

Cong F, Schweizer L, Varmus H. Wnt signals across the plasma membrane to activate the {beta}-catenin pathway by forming oligomers containing its receptors, Frizzled and LRP. Development 2004;131:5103–5115. [PubMed: 15459103]

Deb A, Davis BH, Guo J, Ni A, Huang J, Zhang Z, Mu H, Dzau VJ. SFRP2 regulates cardiomyogenic differentiation by inhibiting a positive transcriptional auto-feedback loop of Wnt3a. Stem Cells 2007;26:35–44. [PubMed: 17916803]

de Iongh RU, Lovicu FJ, Overbeek PA, Schneider MD, Joya J, Hardeman ED, McAvoy JW. Requirement for TGFbeta receptor signaling during terminal lens fiber differentiation. Development 2001;128:3995–4010. [PubMed: 11641223]

Faber SC, Robinson ML, Makarenkova HP, Lang RA. Bmp signaling is required for development of primary lens fiber cells. Development 2002;129:3727–3737. [PubMed: 12117821]

Fenteany G, Janmey PA, Stossel TP. Signaling pathways and cell mechanics involved in wound closure by epithelial cell sheets. Curr. Biol 2000;10:831–838. [PubMed: 10899000]

Finch PW, He X, Kelley MJ, Uren A, Schaudies RP, Popescu NC, Rudikoff S, Aaronson SA, Varmus HE, Rubin JS. Purification and molecular cloning of a secreted, Frizzled-related antagonist of Wnt action. Proc. Natl. Acad. Sci. U S A 1997;94:6770–6775. [PubMed: 9192640]

Goto T, Davidson L, Asashima M, Keller R. Planar cell polarity genes regulate polarized extracellular matrix deposition during frog gastrulation. Curr. Biol 2005;15:787–793. [PubMed: 15854914]

Green JB, Davidson LA. Convergent extension and the hexahedral cell. Nat. Cell Biol 2007;9:1010–1015. [PubMed: 17762892]

Grove M, Demyanenko G, Echarri A, Zipfel PA, Quiroz ME, Rodriguiz RM, Playford M, Martensen SA, Robinson MR, Wetsel WC, Maness PF, Pendergast AM. ABI2-deficient mice exhibit defective cell migration, aberrant dendritic spine morphogenesis, and deficits in learning and memory. Mol. Cell Biol 2004;24:10905–10922. [PubMed: 15572692]

Habas R, Dawid IB, He X. Coactivation of Rac and Rho by Wnt/Frizzled signaling is required for vertebrate gastrulation. Genes Dev 2003;17:295–309. [PubMed: 12533515]

Hall A. Rho GTPases and the control of cell behaviour. Biochem. Soc. Trans 2005;33:891–895. [PubMed: 16246005]

Jones C, Chen P. Planar cell polarity signaling in vertebrates. Bioessays 2007;29:120–132. [PubMed: 17226800]

Jones SE, Jomary C. Secreted Frizzled-related proteins: searching for relationships and patterns. Bioessays 2002;24:811–820. [PubMed: 12210517]

Karner C, Wharton JKA, Carroll TJ. Planar cell polarity and vertebrate organogenesis. Semin. Cell Dev. Biol 2006;17:194–203. [PubMed: 16839790]

Kawano Y, Kypta R. Secreted antagonists of the Wnt signalling pathway. J. Cell Sci 2003;116:2627–2634. [PubMed: 12775774]

Kim SE, Choi KY. EGF receptor is involved in WNT3a-mediated proliferation and motility of NIH3T3 cells via ERK pathway activation. Cell Signal 2007;19:1554–1564. [PubMed: 17374561]

Kreslova J, Machon O, Ruzickova J, Lachova J, Wawrousek EF, Kemler R, Krauss S, Piatigorsky J, Kozmik Z. Abnormal lens morphogenesis and ectopic lens formation in the absence of beta-catenin function. Genesis 2007;45:157–168. [PubMed: 17410548]

Krylova O, Messenger MJ, Salinas PC. Dishevelled-1 regulates microtubule stability: a new function mediated by glycogen synthase kinase-3beta. J. Cell Biol 2000;151:83–94. [PubMed: 11018055]

Ladher RK, Church VL, Allen S, Robson L, Abdelfattah A, Brown NA, Hattersley G, Rosen V, Luyten FP, Dale L, Francis-West PH. Cloning and expression of the Wnt antagonists Sfrp-2 and Frzb during chick development. Dev. Biol 2000;218:183–198. [PubMed: 10656762]

Lescher B, Haenig B, Kispert A. sFRP-2 is a target of the Wnt-4 signaling pathway in the developing metanephric kidney. Dev. Dyn 1998;213:440–451. [PubMed: 9853965]

Liu H, Mohamed O, Dufort D, Wallace VA. Characterization of Wnt signaling components and activation of the Wnt canonical pathway in the murine retina. Dev. Dyn 2003;227:323–334. [PubMed: 12815618]

Liu H, Thurig S, Mohamed O, Dufort D, Wallace VA. Mapping canonical Wnt signaling in the developing and adult retina. Invest. Ophthalmol. Vis. Sci 2006;47:5088–5097. [PubMed: 17065530]

Liu H, Xu S, Wang Y, Mazerolle C, Thurig S, Coles BL, Ren JC, Taketo MM, van der Kooy D, Wallace VA. Ciliary margin transdifferentiation from neural retina is controlled by canonical Wnt signaling. Dev. Biol 2007;308:54–67. [PubMed: 17574231]

Lo WK, Wen XJ, Zhou CJ. Microtubule configuration and membranous vesicle transport in elongating fiber cells of the rat lens. Exp. Eye. Res 2003;77:615–626. [PubMed: 14550404]

Logan CY, Nusse R. The Wnt signaling pathway in development and disease. Annu. Rev. Cell Dev. Biol 2004;20:781–810. [PubMed: 15473860]

Lovicu FJ, McAvoy JW. FGF-induced lens cell proliferation and differentiation is dependent on MAPK (ERK1/2) signaling. Development 2001;128:5075–5084. [PubMed: 11748143]

Lovicu FJ, McAvoy JW. Growth factor regulation of lens development. Dev. Biol 2005;280:1–14. [PubMed: 15766743]

Lyu J, Joo CK. Wnt signaling enhances FGF2-triggered lens fiber cell differentiation. Development 2004;131:1813–1824. [PubMed: 15084465]

Maddala R, Deng P-F, Costello JM, Wawrousek EF, Zigler JS, Rao PV. Impaired cytoskeletal organization and membrane integrity in lens fibers of a Rho GTPase functional knockout transgenic mouse. Lab. Invest 2004;84:679–692. [PubMed: 15094715]

Maddala R, Reddy VN, Epstein DL, Rao V. Growth factor induced activation of Rho and Rac GTPases and actin cytoskeletal reorganization in human lens epithelial cells. Mol. Vis 2003;9:329–336. [PubMed: 12876554]

Maddala R, Reddy VN, Rao PV. Lovastatin-induced cytoskeletal reorganization in lens epithelial cells: role of Rho GTPases. Invest. Ophthalmol. Vis. Sci 2001;42:2610–2615. [PubMed: 11581207]

McAvoy JW. Cell division, cell elongation and distribution of alpha-, beta- and gamma-crystallins in the rat lens. J. Embryol. Exp. Morphol 1978;44:149–165. [PubMed: 650132]

McAvoy JW, Chamberlain CG. Fibroblast growth factor (FGF) induces different responses in lens epithelial cells depending on its concentration. Development 1989;107:221–228. [PubMed: 2632221]

Miller LA, Smith AN, Taketo MM, Lang RA. Optic cup and facial patterning defects in ocular ectoderm beta-catenin gain-of-function mice. BMC Dev. Biol 2006;6:14. [PubMed: 16539717]

Nojima M, Suzuki H, Toyota M, Watanabe Y, Maruyama R, Sasaki S, Sasaki Y, Mita H, Nishikawa N, Yamaguchi K, Hirata K, Itoh F, Tokino T, Mori M, Imai K, Shinomura Y. Frequent epigenetic inactivation of SFRP genes and constitutive activation of Wnt signaling in gastric cancer. Oncogene 2007;26:4699–4713. [PubMed: 17297461]

Olivera-Martinez I, Storey KG. Wnt signals provide a timing mechanism for the FGFretinoid differentiation switch during vertebrate body axis extension. Development 2007;134:2125–2135. [PubMed: 17507413]

Palazzo A, Ackerman B, Gundersen GG. Cell biology: Tubulin acetylation and cell motility. Nature 2003;421:230. [PubMed: 12529632]

Rao PV, Maddala R. The role of the lens actin cytoskeleton in fiber cell elongation and differentiation. Semin. Cell Dev. Biol 2006;17:698–711. [PubMed: 17145190]

Rao V, Wawrousek E, Tamm ER, Zigler S Jr. Rho GTPase inactivation impairs lens growth and integrity. Lab. Invest 2002;82:231–239. [PubMed: 11850536]

Reneker LW, Chen Q, Bloch A, Xie L, Schuster G, Overbeek PA. Chick delta1-crystallin enhancer influences mouse alphaA-crystallin promoter activity in transgenic mice. Invest. Ophthalmol. Vis. Sci 2004;45:4083–4090. [PubMed: 15505059]

Robinson ML. An essential role for FGF receptor signaling in lens development. Semin. Cell Dev. Biol 2006;17:726–740. [PubMed: 17116415]

Rosso SB, Sussman D, Wynshaw-Boris A, Salinas PC. Wnt signaling through Dishevelled, Rac and JNK regulates dendritic development. Nat. Neurosci 2005;8:34–42. [PubMed: 15608632]

Satoh W, Gotoh T, Tsunematsu Y, Aizawa S, Shimono A. Sfrp1 and Sfrp2 regulate anteroposterior axis elongation and somite segmentation during mouse embryogenesis. Development 2006;133:989–999. [PubMed: 16467359]

Schlessinger K, McManus EJ, Hall A. Cdc42 and noncanonical Wnt signal transduction pathways cooperate to promote cell polarity. J. Cell Biol 2007;178:355–361. [PubMed: 17646398]

Schulz MW, Chamberlain CG, de Iongh RU, McAvoy JW. Acidic and basic FGF in ocular media and lens: implications for lens polarity and growth patterns. Development 1993;118:117–126. [PubMed: 7690700]

Shi Y, Bassnett S. Inducible gene expression in the lens using tamoxifen and a GFP reporter. Exp. Eye Res 2007;85:732–737. [PubMed: 17905229]

Smith AN, Miller LA, Song N, Taketo MM, Lang RA. The duality of beta-catenin function: a requirement in lens morphogenesis and signaling suppression of lens fate in periocular ectoderm. Dev. Biol 2005;285:477–489. [PubMed: 16102745]

Stump RJ, Ang S, Chen Y, von Bahr T, Lovicu FJ, Pinson K, de Iongh RU, Yamaguchi TP, Sassoon DA, McAvoy JW. A role for Wnt/beta-catenin signaling in lens epithelial differentiation. Dev. Biol 2003;259:48–61. [PubMed: 12812787]

Tissir F, Goffinet AM. Expression of planar cell polarity genes during development of the mouse CNS. Eur. J. Neurosci 2006;23:597–607. [PubMed: 16487141]

Torres MA, Nelson WJ. Colocalization and redistribution of dishevelled and actin during Wnt-induced mesenchymal morphogenesis. J. Cell Biol 2000;149:1433–1442. [PubMed: 10871283]

Uren A, Reichsman F, Anest V, Taylor WG, Muraiso K, Bottaro DP, Cumberledge S, Rubin JS. Secreted frizzled-related protein-1 binds directly to Wingless and is a biphasic modulator of Wnt signaling. J. Biol. Chem 2000;275:4374–4382. [PubMed: 10660608]

Voiculescu O, Bertocchini F, Wolpert L, Keller RE, Stern CD. The amniote primitive streak is defined by epithelial cell intercalation before gastrulation. Nature 2007;449:1049–1052. [PubMed: 17928866]

Wahl MB, Deng C, Lewandoski M, Pourquié O. FGF signaling acts upstream of the NOTCH and WNT signaling pathways to control segmentation clock oscillations in mouse somitogenesis. Development 2007;134:4033–4041. [PubMed: 17965051]

Wallingford JB, Habas R. The developmental biology of Dishevelled: an enigmatic protein governing cell fate and cell polarity. Development 2005;132:4421–4436. [PubMed: 16192308]

Yun MS, Kim SE, Jeon SH, Lee JS, Choi KY. Both ERK and Wnt/beta-catenin pathways are involved in Wnt3a-induced proliferation. J. Cell Sci 2005;118:313–322. [PubMed: 15615777]

Zandy NL, Playford M, Pendergast AM. Abl tyrosine kinases regulate cell cell adhesion through Rho GTPases. Proc. Natl. Acad. Sci. U S A 2007;104:17686–17691. [PubMed: 17965237]

Zhao H, Yang T, Madakashira BP, Thiels CA, Bechtle CA, Garcia CM, Zhang H, Yu K, Ornitz DM, Beebe DC, Robinson ML. Fibroblast growth factor receptor signaling is essential for lens fiber cell differentiation. Dev. Biol 2008;318:276–288. [PubMed: 18455718]

Zhou CJ, Lo WK. Association of clathrin, AP-2 adaptor and actin cytoskeleton with developing interlocking membrane domains of lens fiber cells. Exp. Eye. Res 2003;77:423–432. [PubMed: 12957142]

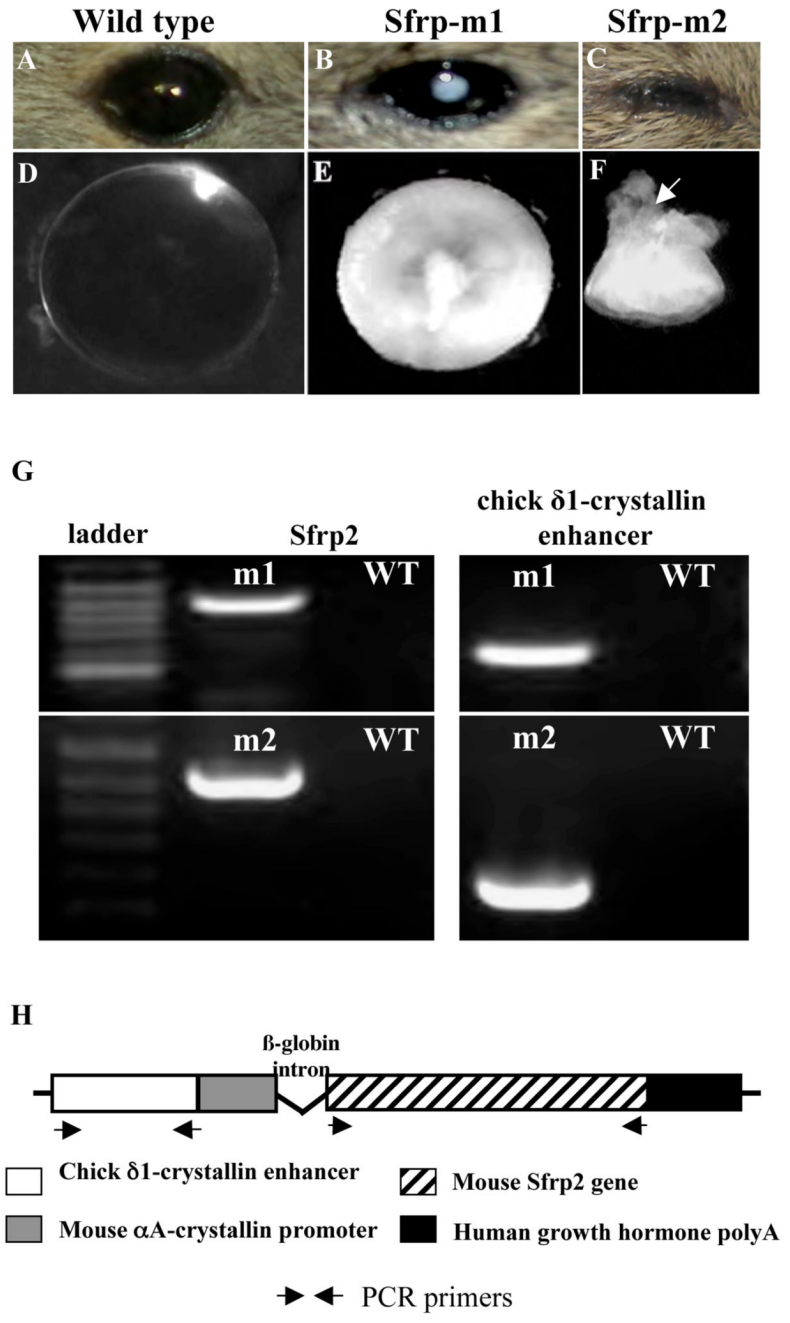

Fig. 1.

Gross morphology of Sfrp2 transgenic lenses. (A) At P21 wild type (WT) littermate eyes were normal and clear. (B) In the Sfrp2-m1 line, the eye looked smaller than the WT and showed distinct and severe bilateral cataract. (C) The eye of the Sfrp2-m2 line did not open. (D, E) At P5, the lens in the WT littermate was transparent, whereas in the Sfrp2-m1 line, the lens was smaller and opaque. (F) In the Sfrp2-m2 line, the lens had an abnormal shape and showed that some fiber cells had extruded from the capsular bag (arrow). The lens was also opaque and much smaller than the WT lens. (G) RT-PCR with total RNA from Sfrp2 transgenic (m1 and m2) and WT littermate lenses at P5 showed that the *Sfrp2* transgene (910 bp) was expressed in the lenses of both Sfrp2-m1 and Sfrp2-m2 mice, but not in WT lenses. PCR using genomic

DNA from crude tail digests was performed to detect the δ1-crystallin enhancer and distinguish transgenic from WT progeny in litters from heterozygotic Sfrp2 mice matings.

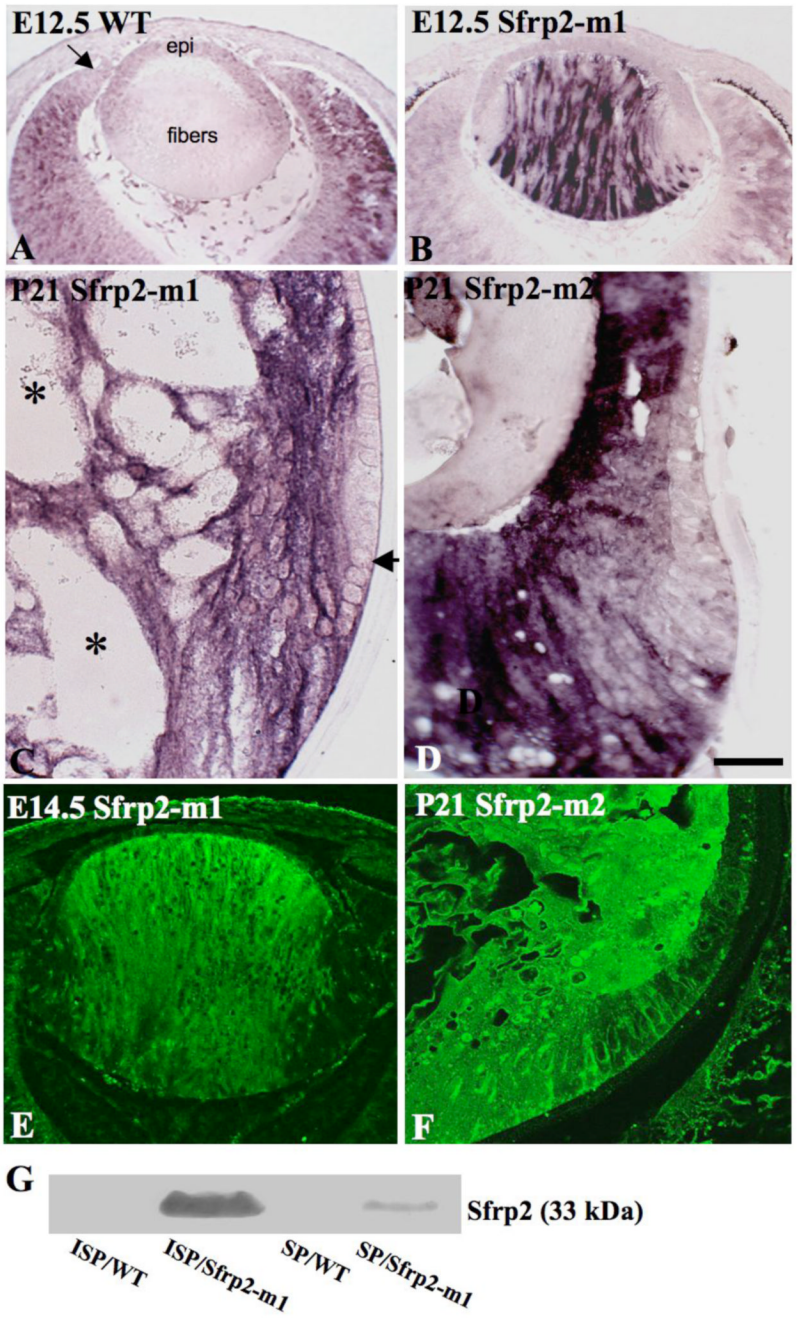

Fig. 2.

Sfrp2 expression patterns in transgenic lenses. *Sfrp2* gene expression was detected by in situ hybridization using a DIG-labeled Sfrp2 riboprobe (A–D). (A) In the WT lens, at E12.5, Sfrp2 mRNA was expressed in the presumptive lens epithelium, but not in the primary fibers. It was expressed throughout most of the optic cup but reduced or absent at its margin (arrowhead in A). (B) In the Sfrp2-m1 lens at E12.5, compared to the WT lens, in addition to weak expression in the lens epithelium, the Sfrp2 mRNA was also prominently expressed in the lens primary fibers. (C) At P21 in the Sfrp2-m1 lens, Sfrp2 mRNA was still strongly expressed in elongating cells at the lens equator and in cortical fiber cells, but not in the degenerated fibers which had lost cell structure (asterisks in C). In the epithelial cells above the lens equator (arrow in C),

Sfrp2 expression was generally undetectable. (D) At P21 in the sfrp2-m2 line, Sfrp2 transcripts were also very strongly detected in the lens fibers, but weak or undetectable in the epithelial cells. (E, F) Sfrp2 protein localization in Sfrp2 lenses was detected by immunohistochemistry using an anti-Sfrp2 antibody. (E) In Sfrp2-m1 lenses at E14.5, Sfrp2 immunoreactivity was strongly detected in the lens fiber cells, but weak or undetectable in the lens epithelial cells. (F) In Sfrp2-m2 lenses at P21, Sfrp2 protein was strongly localized in the elongating cells at the lens equator and in the cortical fiber cells. (G) Western blotting showed that Sfrp2 protein (33 kDa) was present prominently in the insoluble fraction from Sfrp2-m1 lenses at P5. It was also weakly present in the soluble fraction. No Sfrp2 protein was detected in WT lenses at P5. Abbreviations: epi, epithelium; ISP, insoluble protein; SP, soluble protein. Scale bar: Scale bar: 100 μm in A, B, E; 40 μm in C, D, F.

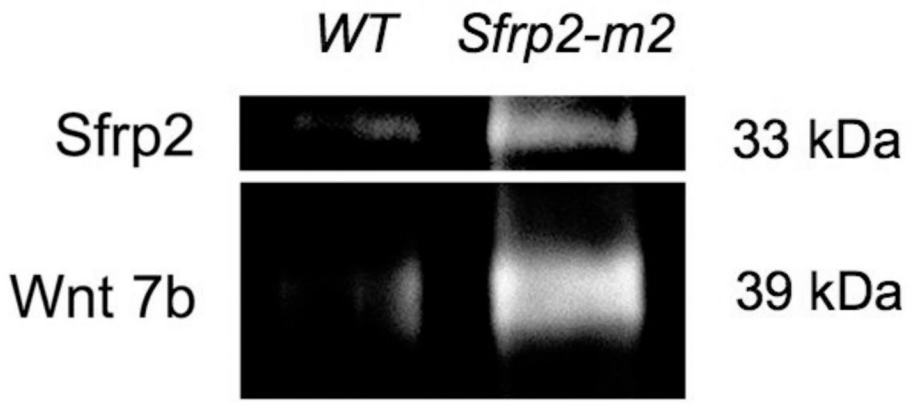

Fig. 3.

Sfrp2 protein co-precipitates with Wnt7b. Sfrp2 was immunoprecipitated from homogenates of lenses from WT and Sfrp2-m2 transgenic mice (P1-3), followed by Western blotting for Sfrp2 and Wnt7b. A strong band for Wnt7b was detected in the Sfrp2-immunoprecipitate from transgenic lenses. In contrast, only traces of Wnt7b and Sfrp2 were detected in the immunoprecipitate from WT lenses.

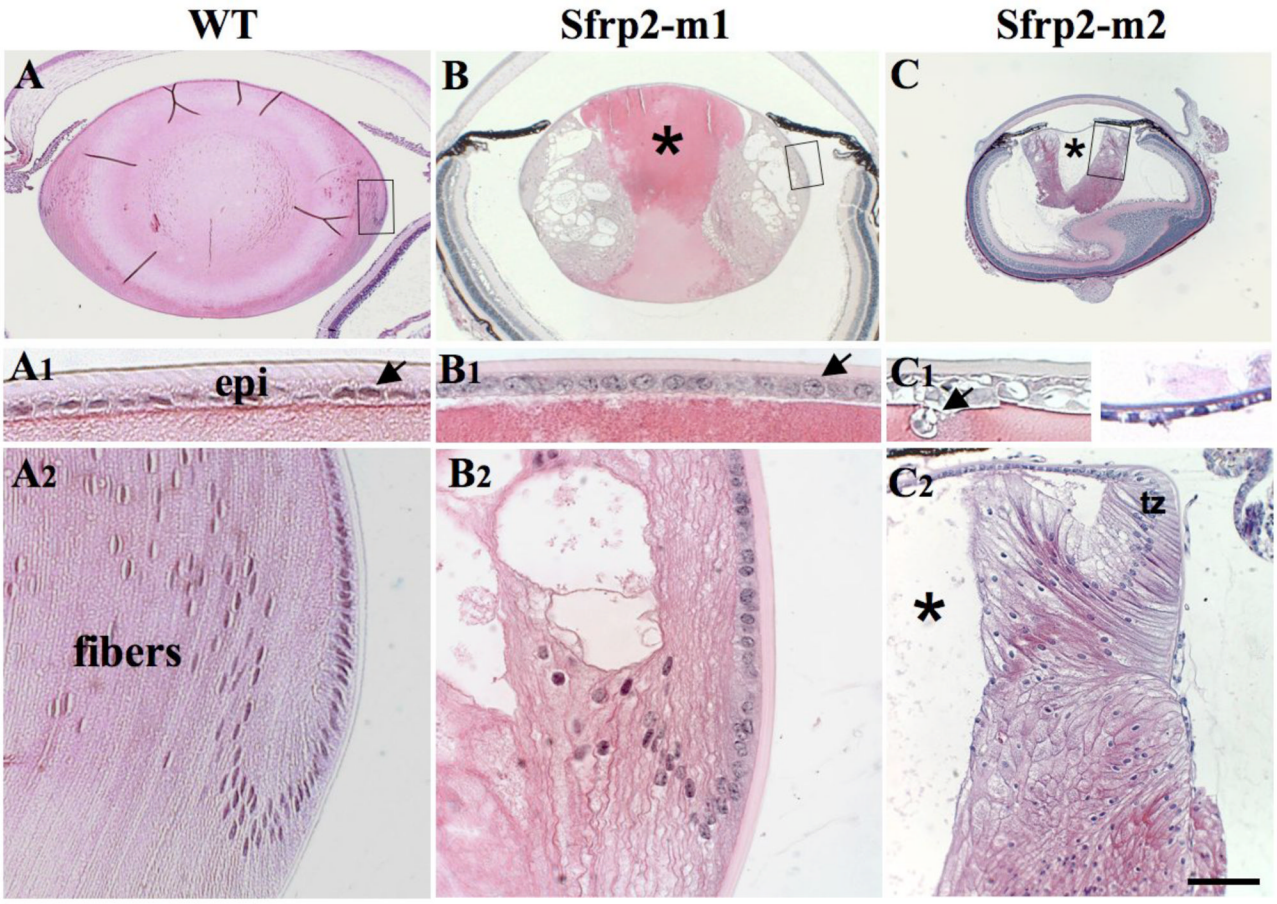

Fig. 4.

Histological analysis of postnatal Sfrp2 transgenic lenses. (A–C) Eyes from P21 Sfrp1-m1 and Sfrp2-m2 transgenic mice along with WT littermates were sectioned and stained with haematoxylin and eosin. (A_1–C_1) Show detail of the lens epithelia and (A_2–C_2) are enlargements of the boxed regions in A–C. (A, A_2) In WT lenses, the elongating and maturing fibers showed orderly alignment along the fiber axis. (B, B_1, B_2) Sfrp2-m1 mice had a severely disrupted lens cellular architecture (asterisk in B). The epithelial cells appeared to be normally arranged but tended to have larger nuclei (arrow in B_1) than in WT lenses (arrow in A_1). In the lens cortex of Sfrp2-m1 mice, where fiber cell maturation occurs, fiber cells often appeared disorganized. Fiber cells were highly vacuolated and, in the innermost region, often had completely broken down. (C) The Sfrp2-m2 lenses were much smaller in size than WT lenses. (C_1) The epithelium was reduced in size and spaces were common between cells. The epithelial phenotype was variable; in most lenses the epithelium remained as a monolayer (right hand image in C_1) but in some lenses the monolayer was disrupted and occasionally cells had migrated into the fiber mass (arrow in left hand image in C_1). (C_2) Fiber differentiation was clearly inhibited and cells in the transitional zone did not elongate sufficiently to reach the overlying epithelium. In the center of the lens a large lumen underneath the epithelium was evident (asterisks in C, C_2). Fiber cells were also disorganized and vacuolated. Abbreviations: epi, epithelium; tz, transitional zone. Scale bar: 100 μm in A–C; 40 μm in $A_{1–2}$, $B_{1–2}$, $C_{1–2}$.

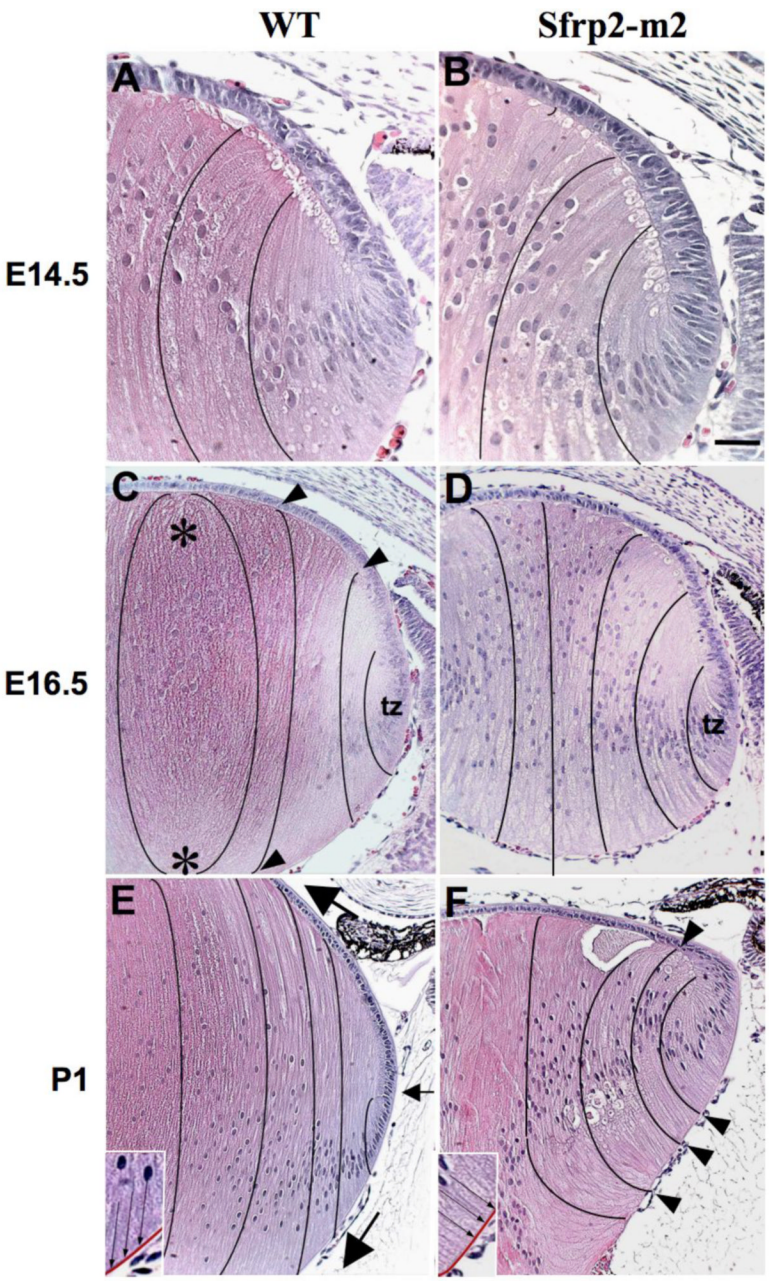

Fig. 5.

Histological analysis of embryonic and neonatal Sfrp2 transgenic lenses. (A–F) Lens sections from E14.5, E16.5 and P1 Sfrp2-m2 transgenic mice and WT littermates were stained with haematoxylin and eosin. (A, B) At E14.5, compared to the WT lens, the lenses in Sfrp2-m2 mice showed essentially normal features in the epithelial and fiber cell compartments. (C, D) At E16.5 the Sfrp2-m2 lenses were slightly smaller than lenses from WT littermates. The fibers in the Sfrp2-m2 lenses appeared to be less closely packed. Moreover, fibers did not curve towards the developing sutures as they did in WT lenses (black lines indicate the curvature of fiber cells in all figures). In WT lenses, the elongating fibers had a concave curvature in the transitional zone but as they moved centrally they progressively developed a convex curvature

(arrowheads in C). When fibers met up with equivalent fibers from an opposing segment of the lens they formed rudimentary sutures (asterisks in C). In the Sfrp2-m2 lenses, the fibers retained a concave curvature and no sutures were evident. (E, F) At P1 in the transitional zone just below the lens equator (small arrow in E) the elongating fibers had a concave curvature but took on a convex curvature as they migrated at their anterior and posterior tips (large arrows) towards the anterior and posterior poles of the lens, respectively. In the sfrp2-m2 lenses, the concave curvature of the fibers was more pronounced than at earlier stages. The elongating fibers in the Sfrp2-m2 lenses remained predominantly at right angles to the posterior capsule and to the epithelium (arrowheads in F). The insets in E and F show more detail of the alignment of the fibers (arrows) and the capsule (red) in WT and Sfrp2-m2 lenses. No sutures formed in the Sfrp2-m2 lenses. Abbreviations: tz, transitional zone. Scale bar: 40 μm in A, B; 50 μm in C–F; 30 μm in insets.

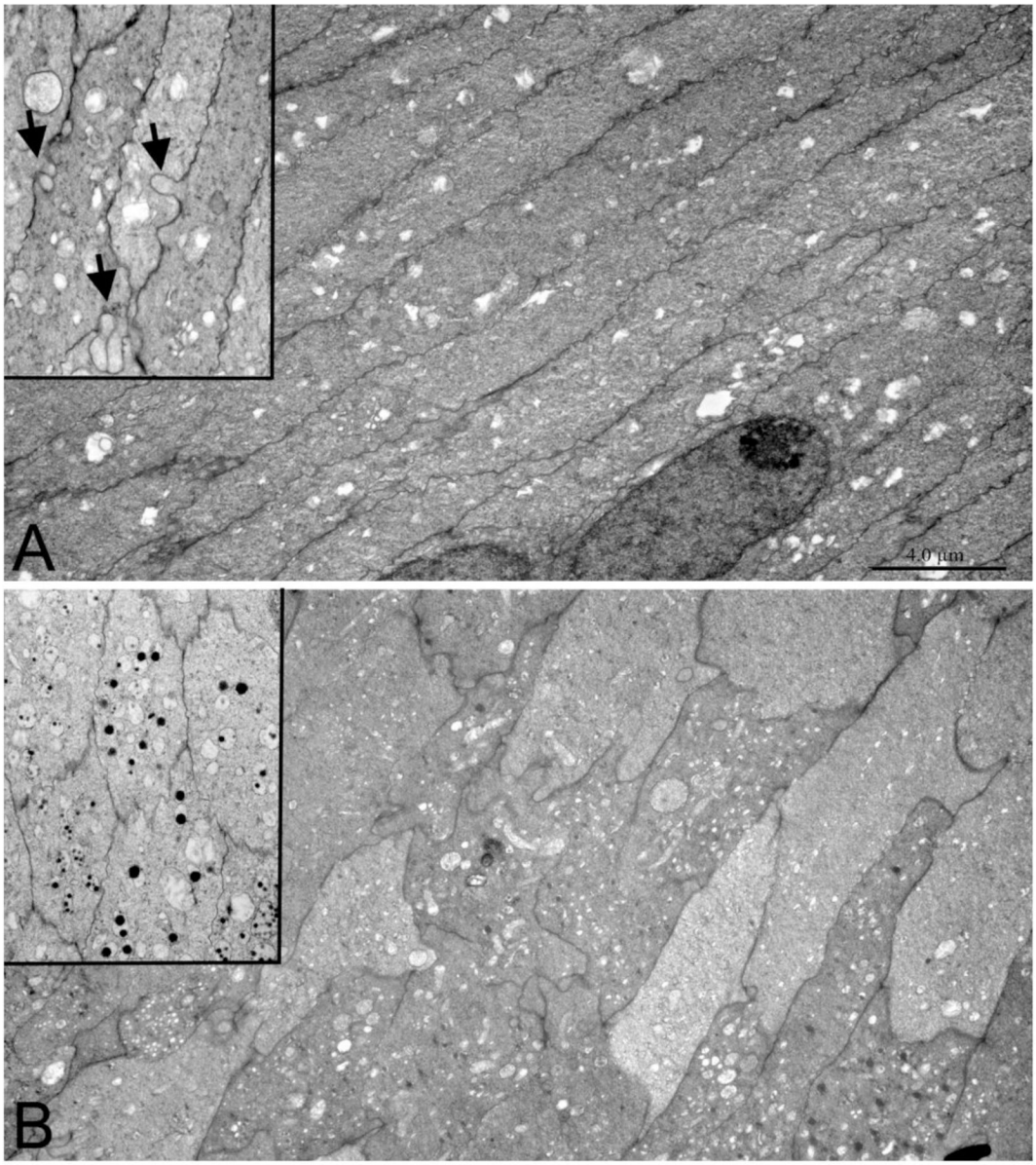

Fig. 6.

Ultrastructural changes in fiber cells in Sfrp2-m2 lenses. (A) At P1 in WT lenses, the elongating fibers in the cortex were clearly well aligned and regularly arranged along the anterior-posterior lens axis. The fiber cells showed interlocking processes, such as ball-and-socket joints (arrows in inset in A). (B) The fibers in the Sfrp2-m2 lenses at P1 were shorter, had irregular shapes and were less regularly aligned than fibers in WT lenses. Interlocking processes were not as abundant in Sfrp2-m2 fibers as in fibers of WT lenses. Small electron dense granules, mostly contained within vesicles, were abundant in some regions of the fibers of Sfrp2-m2 lenses (inset in B) but were not present in WT fibers (inset in A). Scale bar: 4.0 μm.

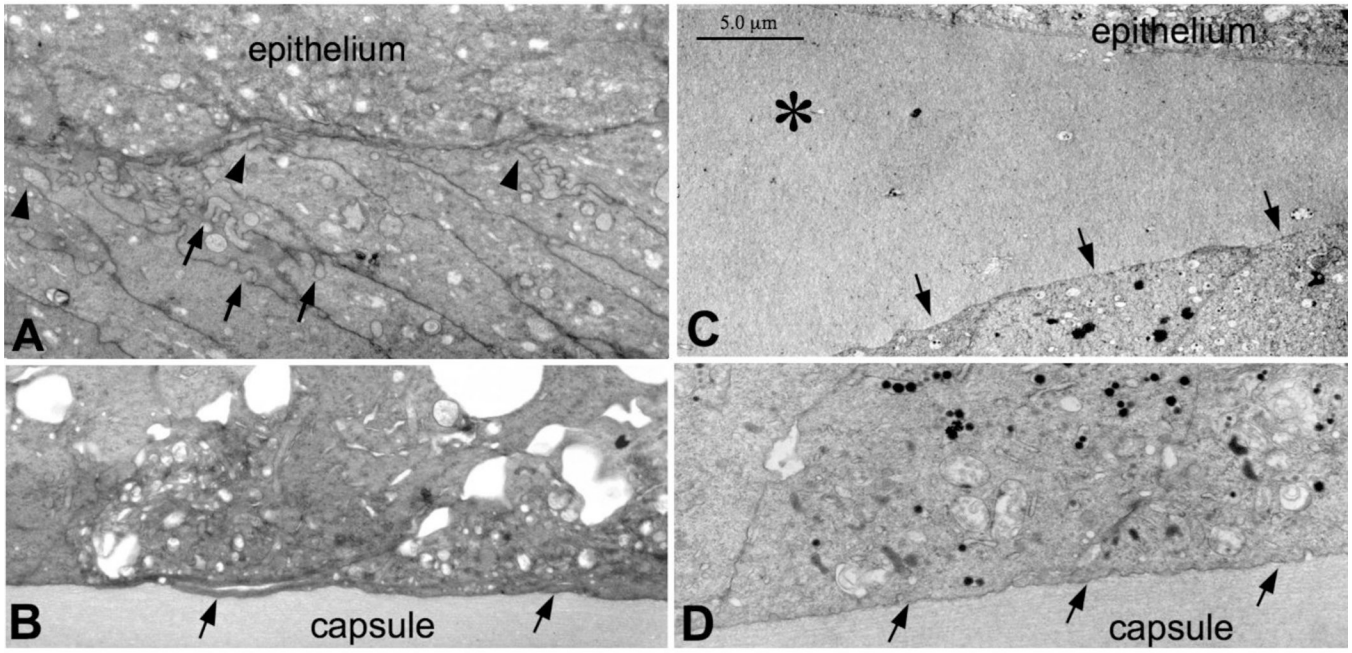

Fig. 7.

Ultrastructural analysis of fiber cell migration in Sfrp2-m2 lenses. (A, B) At P1 in WT lenses, protrusive processes were common at the anterior and posterior tips of the elongating fibers in the lens cortex. Short fiber cell processes extended along the anterior face of the epithelium (arrowheads in A). Interlocking processes between fibers were also abundant in this region (arrows in A). Long filopodia-like processes extended along the posterior capsule (arrows in B). (C, D) In Sfrp2-m2 lenses at P1, fiber elongation was inhibited and in many cases the anterior tips of the fibers did not make contact with the epithelium. This often left a lumen between the epithelium and the fiber mass (asterisk in C). The ultrastructural analysis revealed no evidence of protrusive processes at the anterior or posterior tips of the fibers (arrows in C, D). Scale bar: 5.0 µm

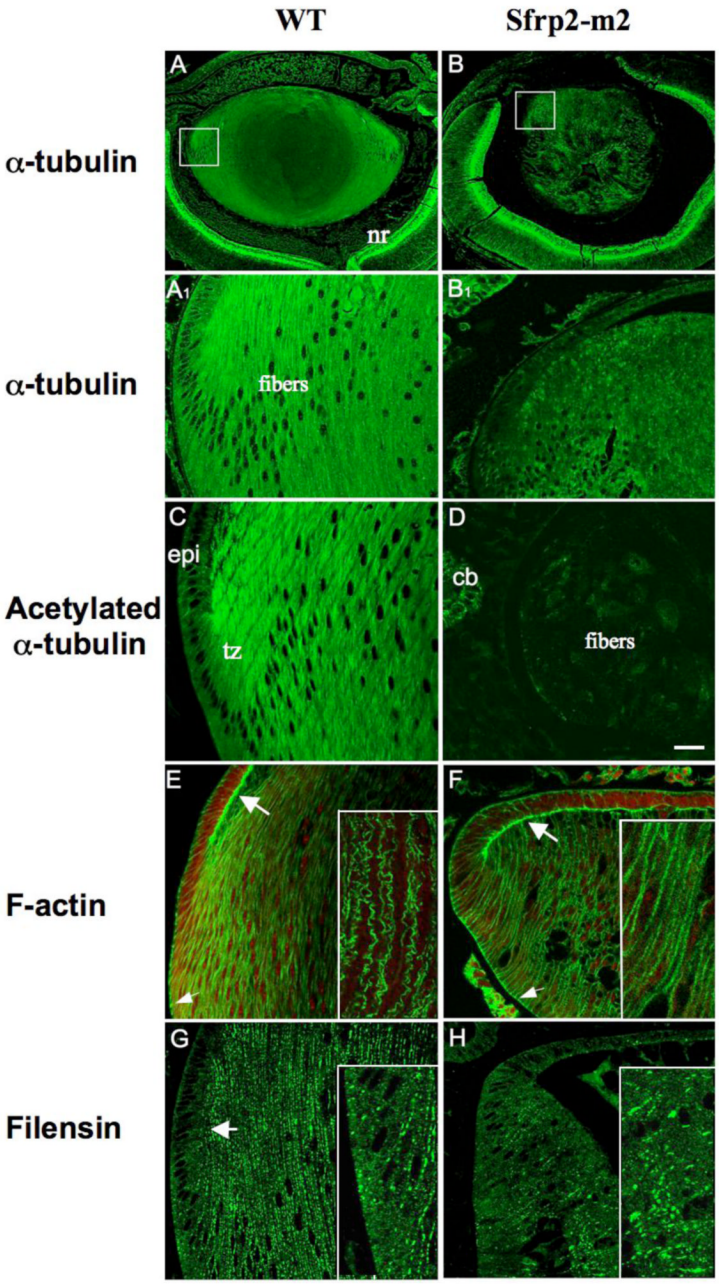

Fig. 8.

Disruption of cytoskeletal architecture in Sfrp2-m2 lenses. (A–H) Immunohistochemistry was carried out to localize α-tubulin, acetylated α-tubulin, F-actin and filensin in P1 lenses. (A) In the WT lens, strong α-tubulin reactivity was evident in the central epithelial cells and outer cortical fibers. It was slightly weaker in the peripheral epithelial cells and the inner cortical and primary fibers. (A_1) Shows the boxed region in A; some alignment of MTs was evident along the elongating fiber axis. (B) In the Sfrp2-m2 lens, α-tubulin reactivity was very weak and patchy in the epithelial cells and fibers. (B_1) Shows the boxed region in B; no MT structure was evident in the disorganized fibers. Similar to WT lenses, Sfrp2-m2 lenses revealed strong α-tubulin reactivity in the neural retina/ciliary body and this served as a useful positive control.

(C) In the WT lens, strong reactivity for acetylated α-tubulin was evident in the outer cortical fibers. Acetylated α-tubulin was weakly detected in the peripheral region of the epithelium but increased during fiber cell elongation in the transitional zone. (D) In lenses of Sfrp2-m2 mice, reactivity for acetylated α-tubulin was very weak and present only in scattered patches. (E) In WT lenses, F-actin was strongly localized in both epithelial cells and fiber cells. Actin filaments were evident along the lateral margins of the cells in the lens cortex, at the epithelial-fiber interface (large arrow) and along the base of the elongating fibers (small arrow). Undulations of the lateral margins of the fibers in the inner cortical region were clearly defined by actin fluorescence (inset in E). (F) In Sfrp2-m2 lenses, fluorescence for F-actin was similar to WT lenses with respect to the strong localization at the epithelial-fiber interface (large arrow) and along the base of the elongating fibers (small arrow). Fluorescence was also prominent along the fiber cell margins but, unlike WT lenses, there were no undulations of the lateral membranes in the Sfrp2 lenses (inset in F). In E and F, cell nuclei were also stained red with propidium iodide. (G, H) Reactivity for filensin was evident at the lens equator in the transitional zone in WT lenses (arrow in G). In the fibers, filensin reactivity was present in prominent tramline-like arrangements that ran along their length (inset in G). In contrast, in the incipient fibers of Sfrp2 lenses, filensin reactivity was present in clumps and showed little tramline-like alignment (inset in H). Abbreviations: epi, epithelium; cb, ciliary body; nr, neural retina; tz, transitional zone. Scale bar: 133 μm in A, B; 25 μm in A_1, B_1, C–H; 5 μm in insets.

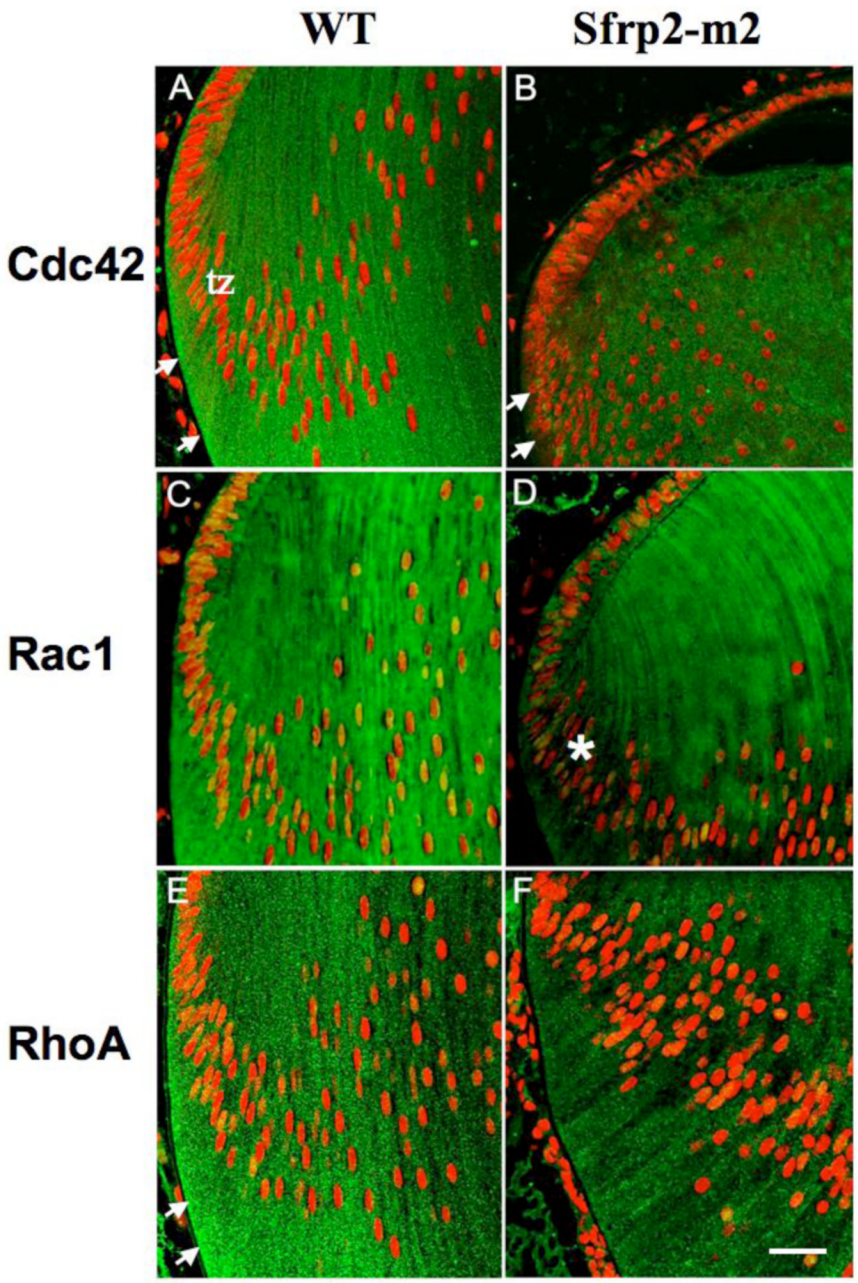

Fig. 9.

Changes in Wnt/PCP signaling components in Sfrp2-m2 lenses. (A–F) Immunohistochemistry was carried out to localize Cdc42, Rac1 and RhoA in P1 lenses. Propidium iodide was also used to stain nuclei red. (A) In WT lenses, Cdc42 was strongly localized in lens epithelial cells and cortical fiber cells. Reactivity was particularly strong at the basal ends of the elongating fibers in the transitional zone at the lens equator (arrows in A). In the more mature fibers in the lens nucleus, Cdc42 reactivity was weaker. (B) In Sfrp2-m2 lenses, Cdc42 reactivity was patchy and was barely detectable at the basal ends of the elongating fibers at the lens equator (arrows in B). (C) In WT lenses, Rac1 was strongly localized in the lens epithelial cells and throughout all the fiber cells. Rac1 reactivity was also present in some of the fiber cell nuclei.

(D) In Sfrp2-m2 lenses, Rac1 reactivity was present throughout the lens but was generally weaker in the elongating cells at the lens equator (asterisk in D). (E) In WT lenses RhoA reactivity was particularly prominent in the basal regions of elongating fibers at the lens equator (arrows in E). (F) In Sfrp2-m2 lenses RhoA immunoreactivity was generally weaker throughout the lens compared with the WT. Abbreviations: tz, transitional zone. Scale bar: 25 μm.

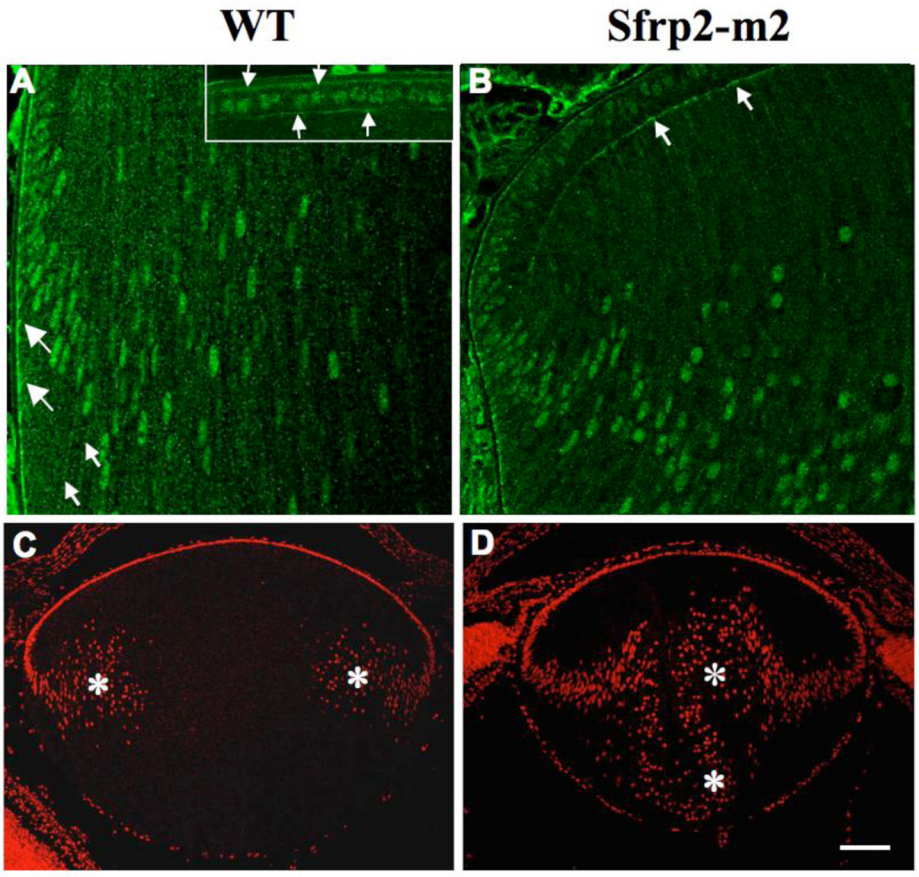

Fig. 10.

pJNK in Sfrp2-m2 lenses. (A, B) Immunohistochemistry was carried out to localize pJNK in P1 lenses. (A) pJNK immunoreactivity was localized in the cytoplasm and the nuclei of both lens epithelial and fiber cells in WT lenses. The nuclear reactivity increased in the cells of the equatorial region. Reactivity for pJNK also increased in the baso-lateral region of cells at the lens equator (large arrows in A) and extended along the length of these elongating fiber cells (small arrows in A). Reactivity for pJNK was also evident at the junction of the epithelium and fibers and at the basal region of epithelial cells (arrows in inset in A). (B) In Sfrp2-m2 lenses pJNK cytoplasmic reactivity was generally weaker than in WT littermate lenses; however, pJNK reactivity at the epithelial/fiber junction (arrows in B) and in the nuclei of the fiber cells in Sfrp2-m2 lenses appeared similar to WTs. (C) Propidium iodide nuclear stain showed that in WT lenses nuclei were characteristically lost in the lens cortex (asterisks in C). (D) Abundant retained nuclei were present throughout the Sfrp2-m2 lenses (asterisks in D). Scale bar: 133 μm in C; 100 μm in D; 25 μm in A, B.

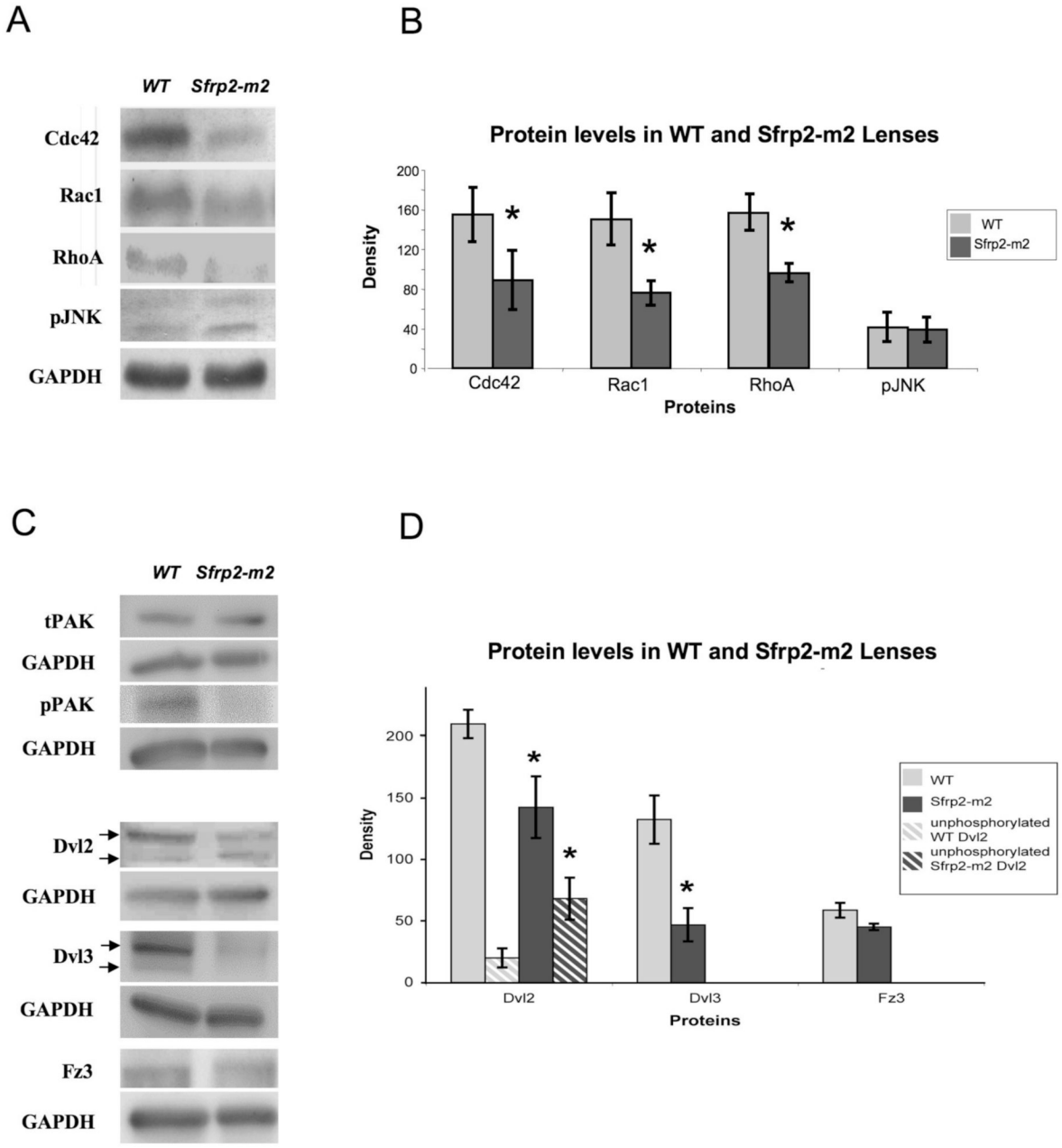

Fig. 11.

Western blot analysis of proteins in WT and Sfrp2-m2 lenses. Western blots were conducted on lysates of P5 lenses. (A) The levels of Cdc42, Rac1 and RhoA were reduced in Sfrp2-m2 lenses compared with WT lenses. Levels of pJNK were similar in WT and Sfrp2-m2 lenses. GAPDH was used as a protein loading control. (B) Band densities were measured for the various proteins in WT and Sfrp2-m2 lenses and standardized with the GAPDH loading control. Data from three separate runs showed that these differences were significant with p=0.013, p=0.014, p=0.017 for Cdc42, Rac1 and RhoA, respectively (asterisks). However, levels of pJNK were not significantly different between Sfrp2-m2 and WT lenses. (C) The level of the GTPase effector, phospho-PAK (pPAK), in Sfrp2-m2 lenses was distinctly reduced compared

to WT lenses, whereas total PAK (tPAK) was similar. Both Dvl2 and Dvl3 showed two bands (arrows) with the upper being the phosphorylated (active) form and the lower being the unphosphorylated (inactive) form. In Sfrp2-m2 lenses for both Dvl2 and Dvl3 the active band was reduced and for Dvl2 the inactive band was increased, compared with WTs. Fz3 appeared similar in Sfrp2-m2 and WT lenses. A GAPDH loading control was included for each comparison. (D) Band densities were measured in at least three separate runs for Dvl2, Dvl3 and Fz3 in WT and Sfrp2-m2 lenses and each measurement was standardized with its GAPDH loading control. Significant differences were detected in active ($p=0.035$) and inactive ($p=0.031$) Dvl2 between WT and Sfrp2-m2 lenses. No significant difference was detected in total (active and inactive combined) Dvl2 ($p=0.363$) between WT and Sfrp2 lenses. There was a significant difference in active Dvl3 ($p=0.011$) between WT and Sfrp2-m2 lenses. For Fz3, no significant difference was detected ($p=0.052$) between WT and Sfrp2-m2 lenses.

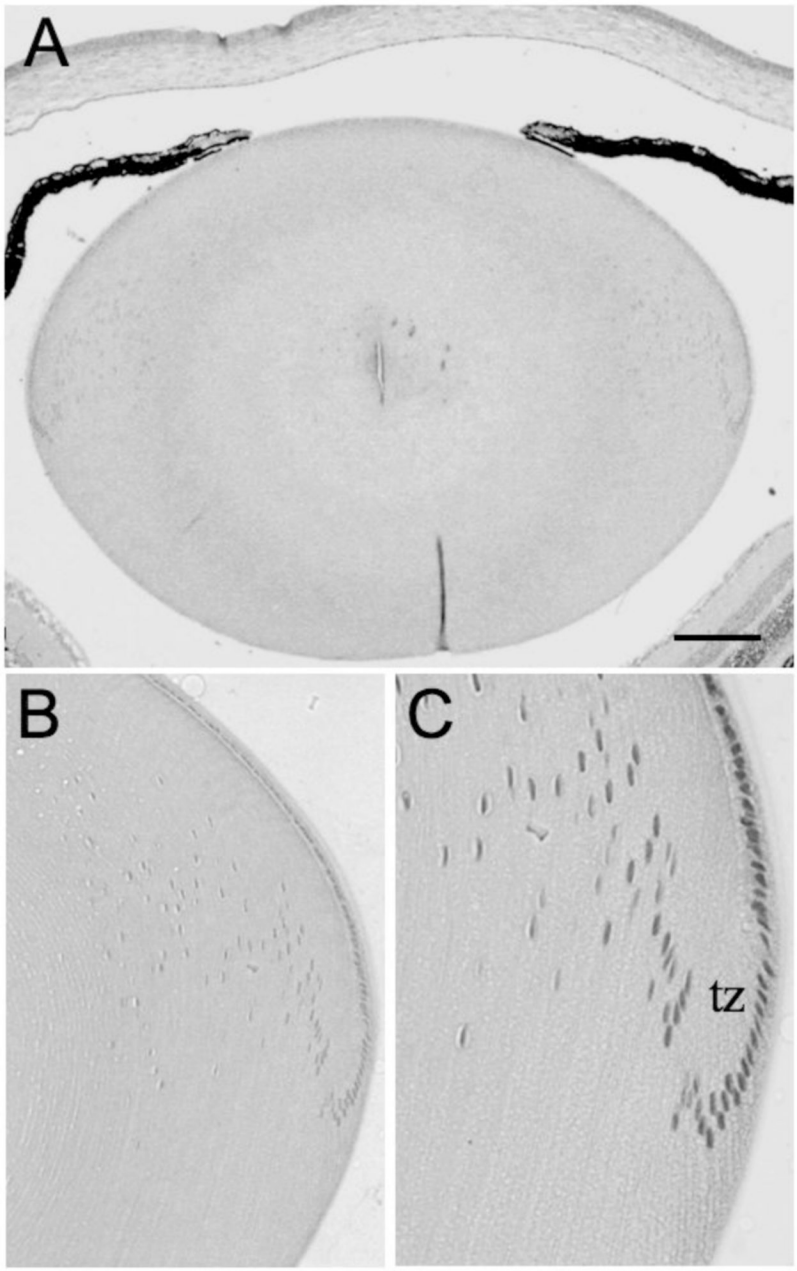

Fig. 12.

The morphology of Sfrp2 mutant lenses. (A–C) A detailed histological analysis of the lenses of Sfrp2 mutant mice revealed no lens defects or abnormalities. (A) At p21 the lens was seen to have normal structure and curvature. (B, C) At higher magnifications the transitional zone at the lens equator was seen to be normal with fiber cells elongating and developing appropriate curvature. Abbreviation: tz, transitional zone. Scale bar: 100 μm in A; 50 μm in B; 25 μm in C.